

## The embryonic and larval development of *Pollimyrus isidori* (Mormyridae, Osteoglossomorpha): its staging with reference to structure and behaviour

Die Embryonal- und Larvalentwicklung von *Pollimyrus isidori* (Mormyridae, Osteoglossomorpha): Stadieneinteilung auf der Basis von Strukturen und Verhaltenselementen

Salif Diedhiou<sup>1</sup>, Peter Bartsch<sup>2</sup> & Frank Kirschbaum<sup>1,3</sup>

<sup>1</sup> Humboldt University, Faculty of Agriculture and Horticulture, Institute of Animal Sciences, Philippstr. 13, D-10115 Berlin, Germany

<sup>2</sup> Museum für Naturkunde der Humboldt-Universität zu Berlin, Invalidenstr. 43, D-10115 Berlin, Germany

<sup>3</sup> Leibniz-Institute of Freshwater Ecology and Inland Fisheries, Müggelseedamm 310, D-12587 Berlin, Germany; frank.kirschbaum@staff.hu-berlin.de (corresponding author)

**Summary:** Descriptive information on the early development of mormyrids is still scarce. In this study, embryos and larvae of laboratory-reared *Pollimyrus isidori* are described. The early ontogeny of this egg-guarding species is documented from the newly spawned egg until the early juvenile stage. Fertilized, demersal eggs are non adhesive, spherical (2 mm), yellow and translucent. At a constant water temperature of 27 °C, cleavage of the blastodisc is finished in about seven hours. The epiboly lasts ten hours. During epiboly, the embryonic shield is distinguished by about 20% yolk cell coverage. Somatogenesis starts when epiboly is almost concluded. Heart beats are detected 35 hours after fertilization soon followed by the first trunk and tail contractions. Hatching occurs about 62 hours after spawning, when the free embryos (or yolk-sac larvae) measure about 3.4 mm. Development of many organ systems of the just-hatched free embryos is not far advanced and in many respects (eye, vascular fin fold network) lags behind those of mormyrid species showing no parental care. After another 10 to 11 days, the larvae start feeding exogenously, when total length reaches 8.9 mm. Since the yolk is completely resorbed only until two or three days later, there is a period of combined endogenous and exogenous food supply. The larval period is characterized by sequential formation of the fins and terminates with the total regression of the fin fold. The caudal and then the pectoral fins develop first, followed by the concomitant emergence of the unpaired fins. Fin differentiation ends with the completion of pelvic fin ray development after almost complete disappearance of the embryonic fin fold. This pattern seems to correspond to that in other Mormyridae, though the sequence may be extended or shifted in relation to other developmental traits. The larval period is never completed before 30 days after oviposition. The fully transformed juvenile with complete squamation is reached on the 60<sup>th</sup> day after spawning and measures around 30 mm in total length. Pronounced growth and differentiation of the cerebellum proceeds during the onset of the free embryonic phase. The study aims at a standard of description of early ontogeny, a basis for future systematic comparison among Mormyridae and Osteoglossomorpha concerning their reproductive biology.

**Key words:** Osteoglossomorpha, Mormyridae, *Pollimyrus*, ontogeny, normal table of development

**Zusammenfassung:** Die Kenntnisse der frühen ontogenetischen Entwicklung der Mormyriden sind immer noch gering. In dieser Studie werden Embryonen und Larven aus Laboraufzuchten der Brutpflegenden Art *Pollimyrus isidori* beschrieben. Die frühe Ontogenese wird vom gerade abgelaichten Ei bis zum frühen Juvenilstadium dokumentiert. Die befruchteten, gelblich-durchscheinenden, demersalen Eier sind nicht klebrig; sie sind rund und haben ca. 2 mm Durchmesser. Bei einer konstanten Wassertemperatur von 27 °C ist die Teilung der Keimscheibe in etwa sieben Stunden abgeschlossen. Die Epibolie dauert zehn Stunden. Während der Epibolie wird der Embryonalschild bei ungefähr 20 % der Dotterumwachsung erkennbar. Die



Somatogenese des Embryos beginnt, wenn die Epibolie fast abgeschlossen ist. Die ersten Kontraktionen des Herzens sind etwa 35 Stunden nach der Befruchtung zu beobachten und werden bald von den ersten Rumpf- und Schwanzbewegungen des Embryos gefolgt. Der Schlupf erfolgt etwa 62 Stunden nach dem Abbläichen, bei einer Totallänge der freien Embryonen (oder Dottersacklarven) von ca. 3,4 mm. Die Entwicklung vieler Organsysteme des Schlüpfings ist gering fortgeschritten und hinkt in vielerlei Hinsicht der Entwicklung der Organe der Mormyriden hinterher, die kein Brutpflegeverhalten zeigen. Dies betrifft zum Beispiel die Augenentwicklung und das kapillare Gefäßnetz des larvalen Flossensaumes. Nach weiteren zehn bis elf Tagen beginnen die Larven bei einer Totallänge von 8,9 mm mit der exogenen Nahrungsaufnahme. Da der Dotter erst zwei bis drei Tage später resorbiert ist, existiert hier eine Periode von kombinierter exogener und endogener Ernährung der Larve. Die larvale Periode ist durch die Sequenz der definitiven Flossenbildung charakterisiert und endet mit der vollständigen Regression des embryonalen Flossensaumes. Zunächst entwickeln sich die Caudalis, dann die Pectorales, gefolgt von der synchronen Entstehung der unpaaren Flossen, Dorsalis und Analis. Die Flossendifferenzierung endet mit der Entwicklung der Bauchflossenstrahlen und dem dann fast vollständig erfolgten Schwinden des embryonalen Flossensaumes. Dieses Muster scheint in der Abfolge dem der anderen Mormyriden zu gleichen, wenn die Sequenz auch im Verhältnis zu anderen Merkmalen in der Entwicklung verschoben sein kann. Die larvale Periode ist bei *P. isidori* nicht vor dem 30sten Tag nach dem Abbläichen abgeschlossen. Das vollständig verwandelte juvenile Stadium mit kompletter Beschuppung wird gewöhnlich erst um den 60sten Tag nach dem Abbläichen und bei einer Gesamtlänge von 30 mm erreicht. Auffällig sind bedeutendes Wachstum und schnelle Differenzierung des Cerebellums während der freien Embryonalphase. Die Studie zielt auf die Entwicklung eines Standards der Beschreibung der frühen Ontogenese als einer notwendigen Basis für den systematischen Vergleich und reproduktionsbiologische Interpretation bei Mormyriden und Osteoglossomorpha.

**Schlüsselwörter:** Osteoglossomorpha, Mormyridae, *Pollimyrus*, Ontogenese, Normentafel der Entwicklung

## 1. Introduction

The Osteoglossomorpha are considered a basal taxon of teleostean fishes (HILTON 2003). They represent a very diverse group comprising six families. With the exception of the Mormyridae, each consists just of a few species or only one species (Pantodontidae, Gymnarchidae). Mormyridae comprise about 200 species (GOSSE 1984). The reproductive and early life history characters of the osteoglossomorphs are quite diverse, too (see recent review of BRITZ 2004) and the phylogenetic significance of single characters (e.g. large oil globules in the egg as seen in *Pantodon buchholzi*) often remains unclear. BRITZ in his paper on *P. buchholzi* also states that "it is surprising how little published information is available on the egg and larval morphology, and early development of other representatives of the Osteoglossomorpha, given the fact that several taxa are economically important food fishes" (BRITZ 2004, p. 215). But even BRITZ (2004) only presents a very brief description of the egg development and the development after hatching up to exogenous

feeding, called larval development in his paper on *P. buchholzi*. We term this stage free embryonic stage according to BALON (1975): egg development or "intrachorionic" embryonic development lasts for about three days in *P. buchholzi*.

This demonstrates that even in novel and particularly useful accounts on the early ontogeny of several groups of lower teleostean fishes, the description is still far behind the analytical depth needed for evaluation of the multitude of morphogenetic events that occur during embryonic and larval development. This usually is caused by limited access and difficult circumstances of acquisition of eggs, embryos, and larvae in these groups. In a similar way the description of the early ontogenetic development of the other osteoglossomorph species described up to now is in general very incomplete, despite some accounts on *Hiodon alosoides* (BATTLE & SPRULES 1960) and *H. tergisus* (SNYDER & DOUGLAS 1978), on *Osteoglossum bicirrhosum* (WOLFSHEIMER 1964, UNGAR 1993); *Scleropages formosus* (AZUMA 1998) and *S. leichhardtii* (LAKE & MIDGLEY 1970, MERREICK & GREEN 1982),



*Heterotis niloticus* (DAGET 1957, HERMENS et al. 2007), *Arapaima gigas* (FONTENELE 1948, 1952, NEVES 1998), *Notopterus notopterus* (MOOKERJEE & MAZUMDAR 1946, AXELROD & BURGESS 1981), *Chitala chitala* (SOUTHWELL & PRASHAD 1919) and *C. ornata* (SMITH 1933), and on *Gymnarchus niloticus* (BUDGETT 1901, ASSHETON 1907, SVENSSON 1933).

More complete descriptions are available for a few species of the Mormyridae: there are data on *Hyperopisus bebe* (JOHNELS 1954), *Pollimyrus adspersus* (KIRSCHBAUM 1987), *Mormyrus rume probosciostris* (SCHUGARDT & KIRSCHBAUM 1996, 2004, 2006), *Campylomormyrus tamandua* (SCHUGARDT & KIRSCHBAUM 1998), *Hippopotamyrus pictus* (KIRSCHBAUM & SCHUGARDT 2002b), and *Petrocephalus soudanensis* (KIRSCHBAUM 2006). The most complete description is found in KIRSCHBAUM & SCHUGARDT (1995) comparing the development of *Pollimyrus adspersus* and *Mormyrus rume probosciostris*. However, in all these articles on mormyrid development and even more so in those on the other osteoglossomorphs the most prominent missing element is a detailed description of the egg or early embryonic development. In the present study we describe for the first time in a very complete manner the ontogenetic development of an osteoglossomorph species, the mormyrid *Pollimyrus isidori* (Valenciennes, 1847), and propose a staging system as orientation for developmental studies.

## 2. Materials and methods

### 2.1. Fishes and experimental tanks

The five adult specimens of *Pollimyrus isidori* (three females and two males) used in this study were captured in Bougouriba River close to Dan, Burkina Faso, in 2005. They were kept in 1080 litres aquaria (200 x 90 x 60 cm) at  $27 \pm 1$  °C and 12L:12D photoperiod. Equipment of aquaria consisted of filter devices, hiding places, and vegetation of the moss *Taxiphyllum* cf. *barbieri* that was used by the male for constructing the nest. Fishes were fed twice a day with live chironomids,

and *Tubifex* worms. The adaptation of the fishes to aquarium conditions lasted about two months. During this period, establishment of territories took place.

Gonad maturation was stimulated with a method developed by SCHUGARDT & KIRSCHBAUM (2004) comprising manipulation of the conductivity of the water alone. The continuous decrease of conductivity was achieved by adding demineralised water to the water in the experimental tank. The water level was maintained constant through an overflow system.

### 2.2. Rearing and documentation systems

Eggs, embryos and larvae described in this study were obtained from nine spawning events of all five fishes. After each spawning event the eggs were isolated from the breeding tank, transferred into Petri dishes (10-20 cm in diameter) or plastic/glass containers (20 x 10 x 6 cm), and finally placed in a thermostat (27 °C, no aeration system) up to exogenous feeding. Larvae were fed in the first three days with newly hatched *Artemia* nauplii. Later on (fourth day of feeding), food supply was supplemented by older *Artemia* nauplii followed by small pieces of *Tubifex*. With growth the larvae had to be separated, the water more often exchanged and well aerated to avoid the notorious losses due to aggression and inflicted wounds followed by diverse infectious diseases.

*In vivo* observations on embryos and larvae were made either with a Wild M-5 stereomicroscope fitted with a Canon PC1048 micro-camera or with a Leica S6E binocular.

For scanning electron microscopy (SEM), specimens were fixed in 2.5% glutaraldehyde in 0.1 mol/l phosphate buffer (pH 7.3). Following fixation for at least two days, specimens were rinsed in phosphate buffer and transferred through a graded ethanol series into absolute ethanol. After two changes in absolute ethanol, samples were critical-point dried in CO<sub>2</sub>, mounted on aluminium stubs, sputter-coated with gold-palladium alloy, and viewed with a Leo 1450 Vp scanning electron microscope.



### 2.3. Terminology

Ontogeny is a continuous process, but can be subdivided into several hierarchically arranged intervals, delimited by more or less evident saltatory morphogenetic events (see e.g. KENDALL et al. 1983, BALON 1975, 1985, 1999, 2002). The term "stage" is employed here as a group of individuals that are similar with respect to certain characters and accordingly represent a morphologically and ethologically defined interval of the ontogenetic sequence. We have numbered the stages, but also associated them with traditional significant names of phases and periods, because named stages are more flexible and easier to remember or recognized for comparison. We have defined each developmental stage by only one or two morphological criteria, termed 'defining criteria', that, based on current knowledge, are assumed to be fundamental features of mormyrid development in general and serve for comparison with other teleost groups. All other developmental characteristics that occur during a stage and are assumed to be rather species-specific or more variable in shape and relative timing are treated as 'concurrent features'.

We sampled embryos and larvae as often as possible, because identification of developmental thresholds and transitions obviously depends on sampling frequency. Spawning time was taken as the moment of fertilization and the beginning of ontogeny. Time of spawning is used as the time zero in age determination, which is given as hrs:min or days after spawning.

## 3. Results

### 3.1. Embryonic period

#### 3.1.1. Embryonic or "chorioned" phase

##### 3.1.1.1. Cleavage

**Stage 1/egg:** Newly spawned eggs observed at 0:38 are roundish to slightly ovoid in shape (fig. 1 a). They do not stick to a substrate and are covered by a chorion, which encloses a nar-

row perivitelline space; largest equatorial median diameter is 2.00 mm (range 1.97-2.10) in living eggs. The eggs are pale yellow except for the circular, uniformly darkish area at the apex of the egg, which corresponds to the micropylar region. At 1:19, the uncleaved egg displays new features that indicate its bipolar differentiation. A distinct, brownish, bulls-eye pattern appeared at the apex of the egg (fig. 1 b): the blastodisc. Underneath the blastodisc, the cytoplasm, closely attached to the yolk, will participate in the formation of the prospective yolk syncytial layer.

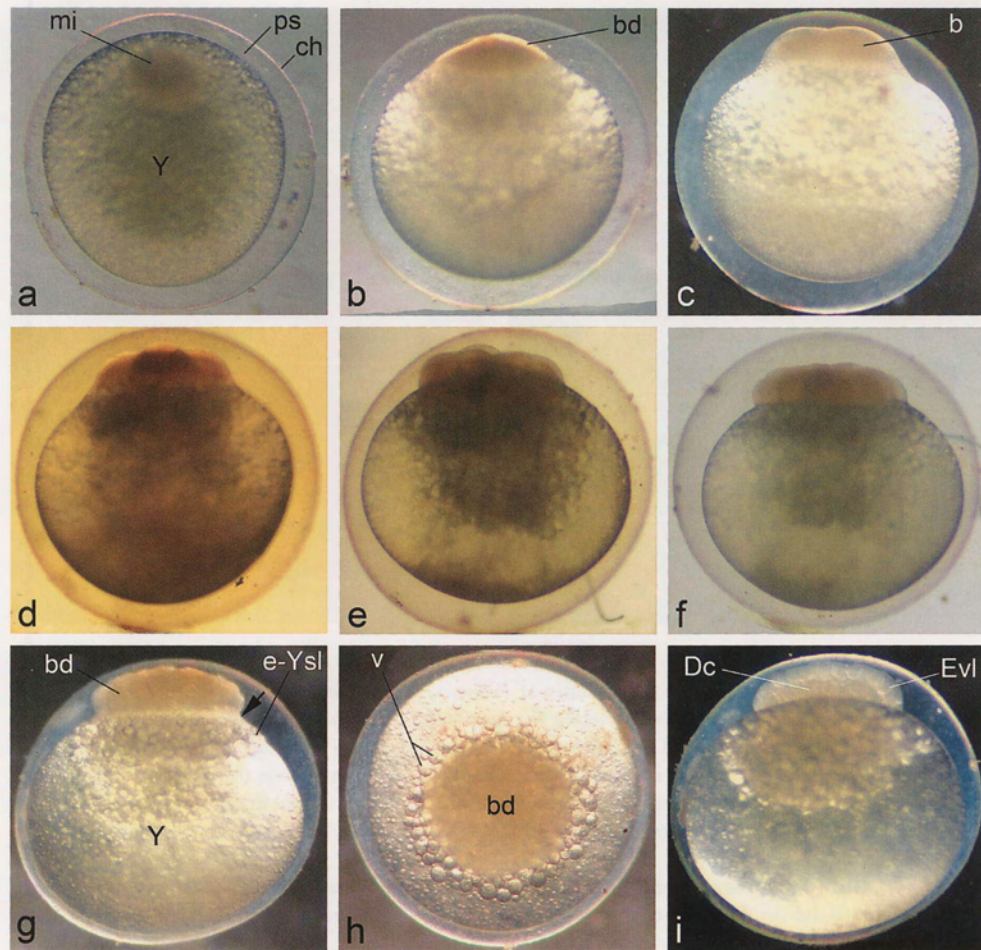
**Stage 2/two-blastomere stage:** The first cleavage furrow starts in the center of the blastodisc and extends downwards to the base of the blastodisc (fig. 1 c, 1:50). The cleavage furrow divides the blastodisc into two approximately equal blastomeres.

**Stage 3/four-blastomere stage:** The second cleavage furrow runs perpendicular to the first one and produces four equal blastomeres (fig. 1 d, 2:50).

**Stage 4/eight-blastomere stage:** The third cleavage consists of two synchronous cleavage furrows orientated perpendicular to the second one, on either side of the first one. The eight blastomeres produced by the third cleavage are arranged in two parallel rows of four cells each (fig. 1 e, 2:50).

**Stage 5/morula:** The subsequent cleavage furrows become asynchronous producing unequal blastomeres in size and intermediate in number between nine and thirty two. The blastomeres form the single layered blastodisc in the early specimens of this stage (Fig. 1 f). In late specimens of this stage (fig. 1 g, 4:05), the blastodisc exhibits a pronounced pebbled appearance and its upper surface may be slightly dome-shaped. It is demarcated from the yolk cell by a ring-like, shallow constriction indicating the formation of the yolk syncytial layer. Three compartments of continuous cortical cytoplasm can be distinguished in the yolk (figs. 1 g, h). (1) A thin, anuclear yolk cytoplasmic layer surrounds the yolk mass at the vegetal pole. (2) The external yolk syncytial layer, located between the yolk cytoplasmic layer and the blasto-

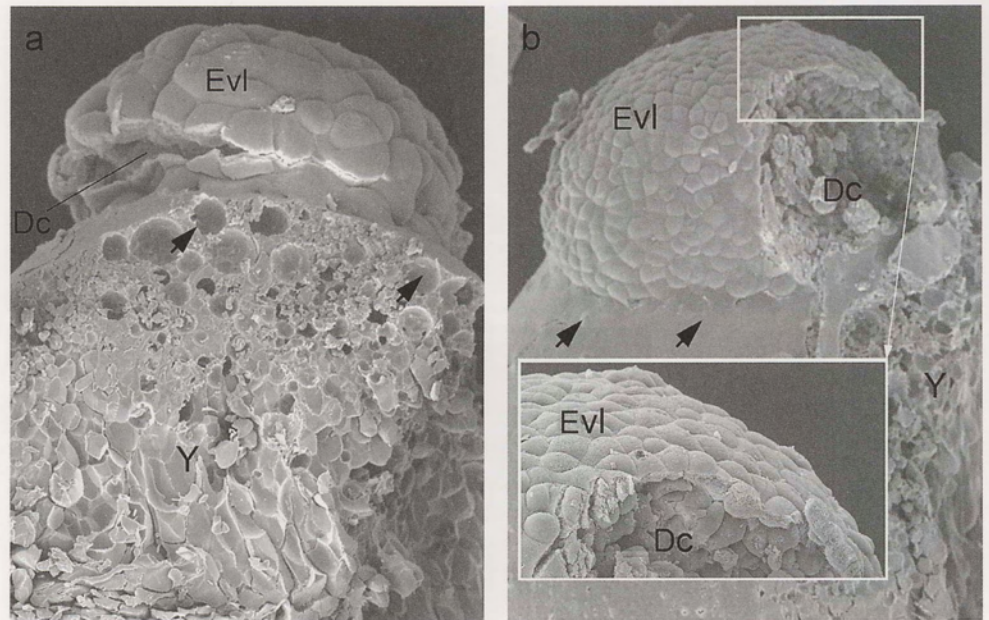




**Figs. 1 a-h:** Cleavage in *Pollimyrus isidori*. (a-b) Stage 1, a newly spawned egg, note micropylar region (mi), chorion (ch), the perivitelline space (ps), and b zygote with forming blastodisc (bd); c stage 2, two cells or blastomeres (b); d stage 3, four cells; (e) stage 4, eight cells; (f-h) stage 5; f early morula with 9-10 cells; g, h late morula with about 28 cells; note the groove (arrow) between the blastodisc (bd) and the yolk sphere (Y) in (g), and the circular external yolk syncytial layer (e-Ysl) with vacuoles (v) slightly different in size and tightly packed in (h); i stage 6, early blastula; note the distinctive large cells of the enveloping layer (Evl) and of the deep cells (Dc). Scale bar: 1 mm.

**Abb. 1 a-h:** Furchung bei *Pollimyrus isidori*. (a-b) Stadium 1, a frisch abgelegtes Ei, beachte die Micropyle (mi), das Chorion (ch), den perivitellinen Raum (ps) und b die Zygote mit entstehender Keimscheibe (bd); c Stadium 2, zwei Zellen oder Blastomeren (b); d Stadium 3, vier Zellen; e Stadium 4, acht Zellen; (f-h) Stadium 5; f frühe Morula mit 9-10 Zellen; g, h späte Morula mit etwa 28 Zellen; beachte die Furche (Pfeil) zwischen der Keimscheibe (bd) und dem Dotter (Y) in (g) sowie die externe syncytiale Dotterschicht (e-Ysl) mit Vakuolen (v) mit etwas unterschiedlicher Größe und dicht gepackt in (h); i Stadium 6, frühe Blastula; beachte die auffälligen großen Zellen der umhüllenden Schicht (Evl) sowie der tiefen Zellen (Dc). Skala: 1 mm.



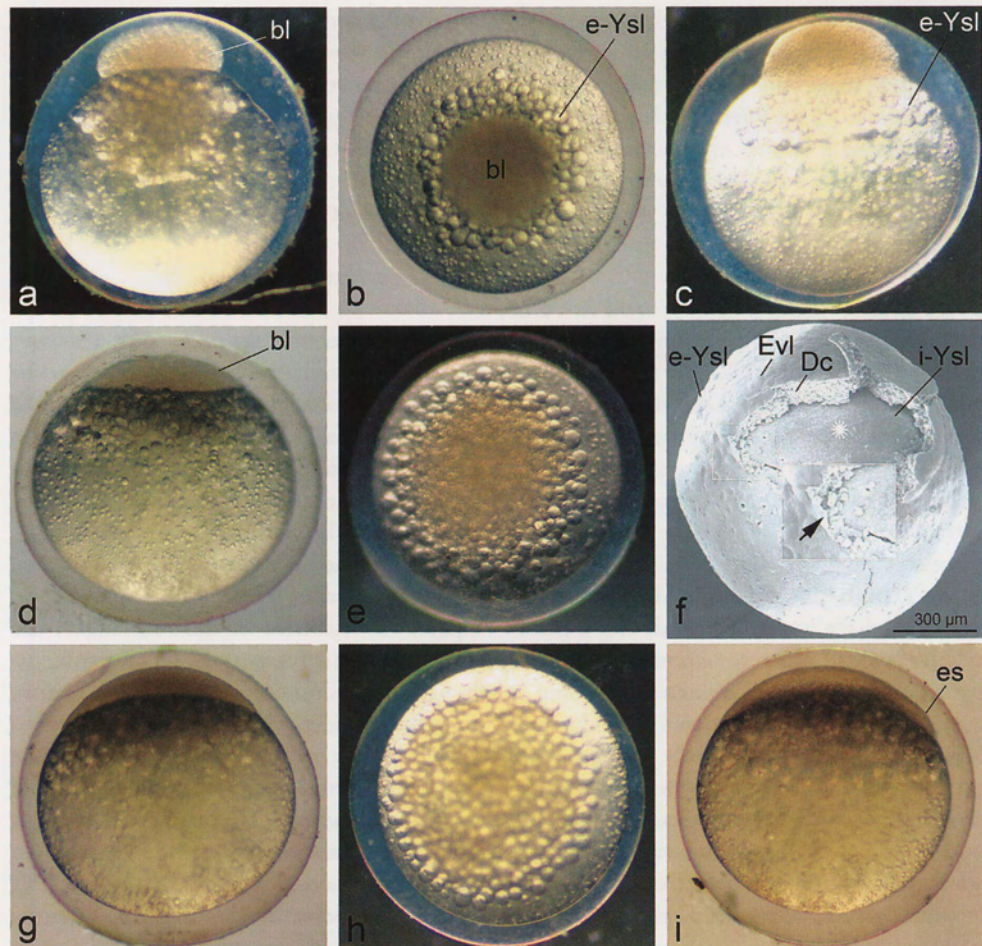


**Figs. 2 a, b:** SEM micrographs of the blastulae of *Pollimyrus isidori*. **a** Stage 6, early blastula with a pebbled surface of the enveloping layer (Evl) covering the deep cells (Dc); note the difference in shape and size between yolk flakes in animal and vegetal pole of the yolk sphere (Y); **b** stage 7, late high blastula; the enveloping layer (Evl) consists of a cohesive layer of surface cells that covers the group of inner tightly packed deep cells (Dc), small interstitial spaces exist between the Dc, irregular in shape and often stretched along the animal-vegetal axis (enlarged framed portion). Y—yolk; arrows point to vacuoles in the yolk syncytial layer. Scale bar: 200 µm.

**Abb. 2 a, b:** REM-Mikrophotos der Blastulae von *Pollimyrus isidori*. **a** Stadium 6, frühe Blastula mit unregelmäßiger Oberfläche der Deckschicht (Evl) die tiefen Zellen (Dc) bedeckend; beachte den Unterschied bezüglich Form und Größe zwischen den Dotterschollen des animalen und vegetativen Poles des Dotters (Y); **b** Stadium 7, späte, hohe Blastula; die Deckschicht (Evl) besteht aus einer zusammenhängenden Schicht von Oberflächenzellen, welche die Gruppe der inneren, dicht gepackten, tiefer liegenden Zellen (Dc) bedecken; kleine, interstitielle Räume existieren zwischen den Dc, unregelmäßig in ihrer Form und oft gestreckt in Richtung der animal-vegetativen Achse (Ausschnitt). Y – Dotter; Pfeile zeigen Vakuolen in der synzytialen Dotterschicht an. Skala: 200 µm.

**Figs. 3 a-i:** Blastulation (**a-f**) and subsequent processes of epiboly and gastrulation (**g-i**) in *Pollimyrus isidori*. **a** Stage 7, early high blastula, the blastoderm (bl) is a roundish mound perched on the top of the yolk with a persisting groove in between; **b** view on the animal pole of specimen in (**a**), note the opaque characteristic of the blastoderm; **c** stage 8, early flat blastula showing a wide and thick belt of the external yolk syncytial layer (e-Ysl), the surface of the blastoderm is smooth but the cells are still distinct; **d, e** stage 10, late blastula or sphere blastula; **d** lens-shaped blastoderm before onset of the proper epiboly (phase II epiboly); **e** view on the animal pole of the specimen in (**d**); note the opaque and translucent appearance of the central and peripheral parts of the blastoderm, respectively, demonstrating their difference in thickness; stage 10 (**f-h**), onset of the proper epiboly; **f** SEM micrograph with partly dissected blastoderm, revealing a thicker central area and thinner margin of globular deep cells (Dc) covered dorsally by the enveloping layer (Evl); the blastoderm covers around 15% of the yolk cell that bulges toward the animal pole taking on a slightly dome shape (asterisk); the enlargement of the framed area shows the attachment of the blastoderm to the yolk mass only by the single layered Evl (arrow); **g** slight demarcation of the blastoderm margin from the yolk margin; **h** view on the animal pole of specimen in (**g**); the external yolk syncytial layer (e-Ysl) is partially covered by the vegetally expanding blastoderm; note the transparency of





the central area of the blastoderm due to its thinning and revealing also the vacuoles of the internal yolk syncytial layer (i-Ysl); i Stage 11, embryonic shield (es) on the germ ring (gr). Scale bar: 1 mm.

**Abb. 3 a-i:** Blastulation (a-f) und nachfolgend die Prozesse von Epibolie und Gastrulation (g-i) bei *Pollimyrus isidori*. a Stadium 7, frühe, hohe Blastula, das Blastoderm (bl) ist ein runder Hügel aufgepflanzt auf der Spitze des Dotters mit einem persistierenden Spalt dazwischen; b Sicht auf den animalen Pol des Keimes in (a); beachte das opake Erscheinungsbild des Blastoderms; c Stadium 8, frühe, flache Blastula mit einem weiten und dicken Ring der äußeren syncytialen Dotterschicht (e-Ysl); die Oberfläche des Blastoderms ist zwar glatt, die Zellen aber sichtbar; Stadium 10 (d, e), späte Blastula oder sphärische Blastula; d linsen-ähnliches Blastoderm vor dem Beginn der eigentlichen Epibolie (Phase II der Epibolie); e Sicht auf den animalen Pol des Keims in (d); beachte die opake und durchscheinende Erscheinung des zentralen und peripheren Teils des Blastoderms, beziehungsweise den Unterschied in der Dicke; Stadium 10 (f-h), Beginn der eigentlichen Epibolie; f REM Mikrophoto mit teilweise freigelegtem Blastoderm; beachte eine dickere, zentrale Zone und einen dünneren Rand globulärer tiefer Zellen (Dc), die dorsal von einer Deckschicht (Evl) umgeben sind; das Blastoderm bedeckt rund 15% des Dotters der sich zum animalen Pol hin erstreckt und eine kuppelartige Form ausbildet (Sternchen); der vergrößernde Ausschnitt zeigt die Anheftung des Blastoderms an den Dotter durch eine einschichtige, tiefe Lage der Deckschicht (Evl) (Pfeil); g leichte Abgrenzung des Blastodermrandes vom Dotterrand; h Sicht auf den animalen Pol des Keims von (g); die äußere, syncytiale Dotterschicht (e-Ysl) ist partiell von dem sich vegetad ausbreitenden Blastoderm bedeckt; beachte die Transparenz der zentralen Zone des Blastoderms, die aus seiner dünnen Schichtung resultiert; die Vakuolen der inneren, syncytialen Dotterschicht sind auch sichtbar; i Stadium 11, Embryonalschild (es) auf dem Keimring (gr). Skala: 1 mm.



derm rim, is a relatively thick belt of cytoplasm populated by the yolk syncytial nuclei and accumulated large yolk vacuoles. Beneath the blastoderm is (3) the internal yolk syncytial layer comprising a thinner cytoplasm also populated by the yolk syncytial nuclei.

#### 3.1.1.2. Blastula

**Stage 6/early blastula stage:** For the first time the blastodisc differentiates into two types of cells (fig. 1 i, 4:21; fig. 2 a). The first cell population distinguished is the enveloping layer. It is made up of the most superficial cells of the blastoderm, which form an epithelial sheet a single cell layer thick. Underneath the internal surface of the enveloping layer the deep layer of cells is situated.

**Stage 7/high blastula stage:** At this stage the deep cells have multiplied producing a multicellular layer. As cleavage continues, cell size decreases and cell number increases leading to a higher blastula in the restricted blastodisc area (figs. 2 b, 3 a; 4:44). Externally, a constriction between blastoderm and yolk rich region is still observed. The blastoderm becomes solid and opaque (fig. 3 b). Significant variation in size among the cells of the enveloping layer was no longer observed. Some deep cells start the lobopodial movement whose dominant feature is shortening of their finger-like leading extension (fig. 2 b, frame) pulling the cell body forward vegetally.

**Stage 8/flat blastula stage:** The margin of the blastoderm extends peripherally and the annular groove at the blastoderm-yolk junction disappears (fig. 3 c, 7:55). This change in shape is the most apparent sign that phase I epiboly has started. As epiboly continues the blastoderm thins out considerably leading to a shorter animal-vegetal axis. This is accomplished by the streaming outwards, the surfacing, of the deepest cells of the blastoderm.

**Stage 9/late or sphere blastula stage:** The germ re-establishes the roundish or spherical shape of the newly spawned eggs with a lens-shaped blastoderm (fig. 3 d, 11:12). The animal surface of the yolk cell underlying the blasto-

derm is flat and most of the yolk vacuoles are inside or immediately below the external yolk syncytial layer vegetal to the blastoderm (fig. 3 e). During this stage the solid blastoderm thins and becomes translucent (fig. 3 e). The duration of stages 8 and 9 (3 h 57 min) is nearly as long as the duration of stages 1 to 7 (4 h 44 min).

#### 3.1.1.3. Gastrula

**Stage 10/onset of epiboly proper:** The margin of the blastoderm spreads slightly over the adjacent yolk margin (figs. 3 f, g; 15:30). The cap-shaped blastoderm presents internally a deep cellular layer of almost uniform thickness at the end of this stage. The animal yolk cell surface visibly bulges into the blastoderm, but forms a flattened ledge, on which the marginal deep cells still rest (fig. 3f, frame). There is no apparent contact between the underside of the blastoderm and the surface of the yolk, although there is no obvious cavity either; thus, the yolk is distinctly separated from the blastoderm by a narrow cleft (fig. 3 f). It is mainly the enveloping layer keeping the blastodisc and yolk together mechanically. The blastoderm thins out to become transparent so that the internal yolk syncytial layer becomes entirely visible (fig. 3 h).

**Stage 11/embryonic shield:** During the early part of this stage, the margin of the blastoderm differentiates into the germ ring. Soon, the first sign of the prospective embryonic shield appear as a slight bulge, the dorsal blastopore lip, on the germ ring. As the blastoderm has covered 20% of the yolk, a well visible embryonic shield develops from the blastopore lip (fig. 3 i, 17:37). The longitudinal axis of the future embryo is already defined by that of the embryonic shield. The margin of the blastoderm reaches the vegetal ridge of the external yolk syncytial layer. At the same time, the deep cells migration becomes externally visible for the first time, which explains why the apex of the blastoderm becomes translucent (fig. 3 i).

**Stage 12/evacuation zone:** The blastoderm covers 30% of the yolk surface, as the margin of the blastoderm comes to lie just beyond the lower margin of the external yolk syncytial layer



(fig. 4 a, 17:45). The deep cells from the central area (apex) of the blastoderm migrate rapidly by both, epiboly and convergence toward the embryonic shield axis, leaving an empty space the evacuation zone. The animal surface of the yolk sphere becomes flat. The internal yolk syncytial layer becomes conspicuous underneath the remarkably thin and transparent blastoderm (fig. 4 b).

#### 3.1.1.4. Neurula

**Stage 13/extension:** The blastoderm continues to spread and covers 50% of the yolk surface (fig. 4 c, 18:41). As the blastoderm expands vegetally, the external yolk syncytial nuclei move underneath the blastoderm to distribute over the yolk mass. The embryonic shield becomes inflated and elongated towards the animal pole. It first forms by a thickening, or columnarisation, of the ectodermal epithelium to form a classical neural plate. This process, collectively termed extension, defines the anterior-posterior axis of the future embryo morphologically. The internally depressed and externally inflated evacuation zone is roofed by only the thin and transparent mono-layered epidermal enveloping layer. The vegetal scattering of the yolk vacuoles underneath the blastoderm demonstrates that the yolk syncytial layer has also spread together with the blastoderm over the yolk surface at the same rate.

**Stage 14/early neurula:** The blastoderm covers up to 75% of the yolk surface by the end of this stage (fig. 4 d, 19:43). The embryonic shield continues to lengthen and broaden rostrally. The lateral edges, the neural folds, are already observed in the anterior portion of the neural plate. The evacuation zone, displaced from the vertical axis of the yolk mass becomes narrower and lower.

**Stage 15/wedge-shaped neural plate:** The epibolic spreading of the blastoderm over the yolk extends to 90%, leaving an exposed yolk plug (fig. 4 e, 21:07). The neural plate continues to extend laterally, and becomes wedge-shaped. In the prospective head region, a primary brain cavity is preformed first as a wide shallow groove.

#### 3.1.1.5. Somatogenesis

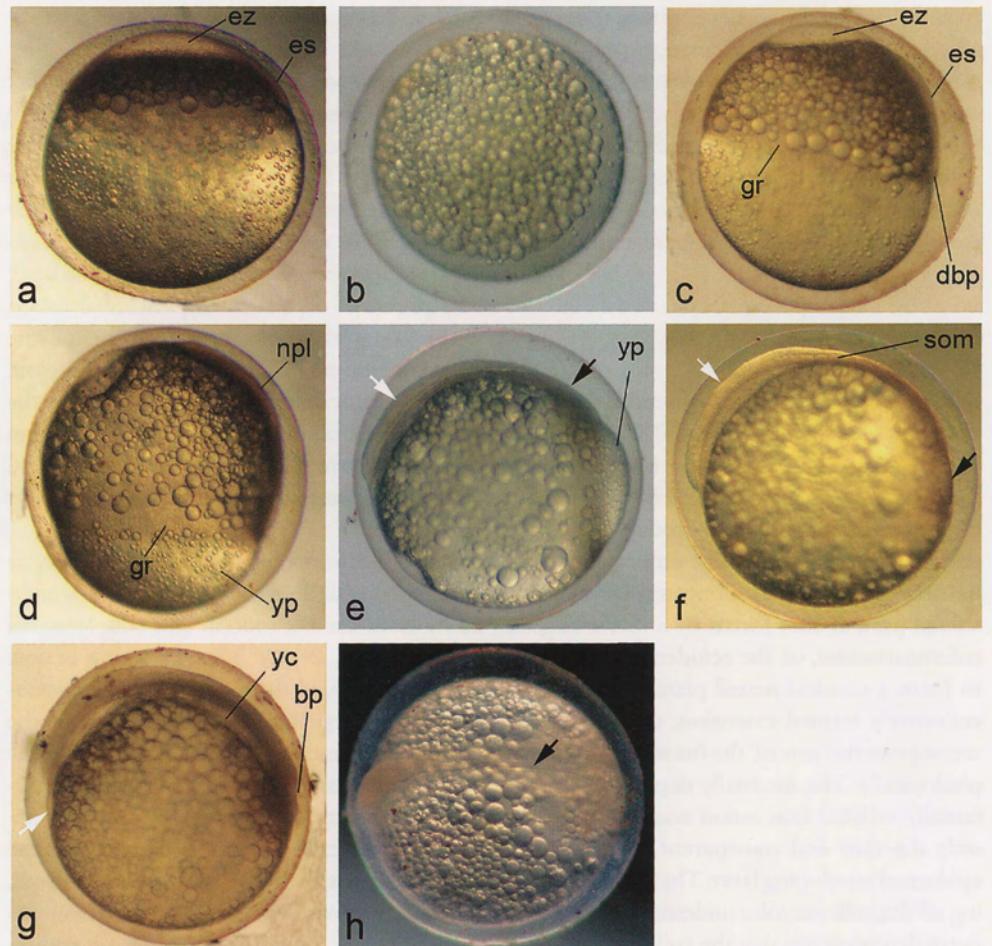
**Stage 16/onset of somatogenesis:** The first somites differentiate in the dorsal mesoderm adjacent to the caudal end of the prospective head (fig. 4 f, 23:57). The neural folds of the prospective head region are elevated from the epidermal yolk sac cover. A depression has started to form in the yolk mass underlying the head: The primary yolk cavity or pericardial cavity. The notochord becomes visible at the midline of the neural plate excluding the head region. Yolk coverage is not completed yet, but the exposed yolk no longer protrudes as the germ ring contracts to close it up. A small evacuation zone is still present, but is not seen again after this stage.

**Stage 17/latest epiboly stage:** Epiboly is completed and the yolk mass is wholly wrapped by both the blastoderm and yolk syncytial layer (fig. 4 g, 24:42). The germ ring is now swollen all around the almost occluded blastopore by a deep areolar concentration of the prospective mesoderm, which is thickest at the dorsal blastopore lip. The primary yolk sac cavity extends further rostrally and caudally underneath the entire neural plate to form the segmentation cavity. As neurulation proceeds, a neural groove becomes evident along the midline of the plate, with a widened, spoon-shaped depression at the anterior end (fig. 4 h).

**Stage 18/blastopore closure stage:** This stage marks the proper end of the epibolic process by the closed blastopore. The neural folds have approached each other along the midline for one third of their length, which causes the neural plate to take a dumbbell-shaped appearance (fig. 5 a, 25:52). In the prospective head region, the neural folds become thick. Mesodermal material has concentrated at the closed blastopore, and will differentiate into the rudimentary trunk-tail bud in the following stage.

**Stage 19/early trunk-tail bud stage:** The lateral edges of the neural plate are prominent and fold in toward the midline of the embryo, mainly in the prospective trunk-tail region (fig. 5 b, 27:21). The most caudal portion of the





**Figs. 4 a-h:** Embryonic development of *Pollimyrus isidori*. Stage 12 (a, b), evacuation zone (ez); a shows a transparent ez and a flat underlying yolk surface; the central area possibly consists of one-layered deep cells as judged by the high transparency of the central area of the blastoderm; note the embryonic shield (es); b the internal yolk syncytial layer exhibits densely packed vacuoles; c stage 13, 50% epiboly stage, columnarization; the region of the blastoderm where the embryonic shield (es) is localized seems to have advanced further vegetally than the remainder of the blastoderm; the nuclei are still immediately behind the germ ring (gr) and follow the epibolic movement; d stage 14, 75% epiboly stage with onset of neurulation; the yolk plug (yp) is constricted by the flat and short gr; note the high concentration of the vacuoles around the neural plate (npl); yolk under evacuation zone hollowed; e stage 15, stage with wedge-shaped neural plate differentiated into prospective brain (white arrow) and trunk (black arrow) region; f stage 16, embryo, epiboly finished with emergence of the three first somites (som) and presence of the anterior primary yolk cavity/pericardial cavity under the brain region (white arrow); stage 17 (g, h), note the remnant of the evacuation zone (white arrow), g the yolk cavity (yc) underlying the entire neural plate and in h a dorsal view of specimen in (g) showing the spoon-shaped midline region of the neural plate with formed notochord (black arrow). bp—blastopore, dbp—blastopore lip. Scale bar: 1 mm.

**Abb. 4 a-h:** Embryonalentwicklung von *Pollimyrus isidori*. Stadium 12 (a, b), Evakuationszone (ez); a zeigt eine transparente ez und eine flache, darunterliegende Dotteroberfläche; die zentrale Zone scheint aus einer einschichtigen Lage tief liegender Zellen zu bestehen; dies lässt die große Transparenz der zentralen Zone des Blastoderms vermuten; beachte den Embryonalschild (es); b die innere, syncytiale Dotterschicht



neural anlage and underlying mesoderm project from the epidermal yolk sac cover forming a rudimentary trunk-tail bud.

**Stage 20/brain regionalisation:** The neural plate projects rostrally and caudally now beyond the epidermal yolk-sac cover and attains a club-shaped appearance (fig. 5 c, 29:17). A lateral symmetrical thickening of the neural folds suddenly has appeared in the head region. The dorsolateral constriction behind its anterior third illustrates the first indication of a primary brain division into prosencephalic (rostral) and deuterocephalic regions (caudal). The neural groove is deeper due to the uprising neural folds and growing paraxial mesodermal material.

**Stage 21/neural anlage stage:** This stage fully deserves the name embryo in further description up to hatching and demarcates the end of the neurulation process. First the neural folds become contiguous along the dorsal midline of the trunk-tail, then become fused to form a continuous neural rod (fig. 5 d, 32:07). Around 12 somites are differentiated but were not sufficiently discrete at the posterior end to be counted accurately by means of light microscopy.

**Stage 22/heart formation stage:** The presumptive heart tube is visible (fig. 5 e, 33:57). The central nervous system lays in a deep groove formed by the remarkably elevated paraxial mesoderm in the trunk-tail region and the prominent, densely packed mesoderm mass in the head region. From the end of the brain-stem caudally, the spinal cord is bordered by

12 pairs of somites laterally, and further posteriorly by an undifferentiated mass of mesoderm destined for the further differentiation of somites. The caudal tail region of the embryo, in which Kupffer's vesicle appears, is separated from the yolk sac and curved downward along it (fig. 5 e). The forming heart is seen inside the extended pericardial cavity. Three primary subdivisions of the brain into telencephalon plus diencephalon, mesencephalon, and rhombencephalon can be traced by following their ventricular borders.

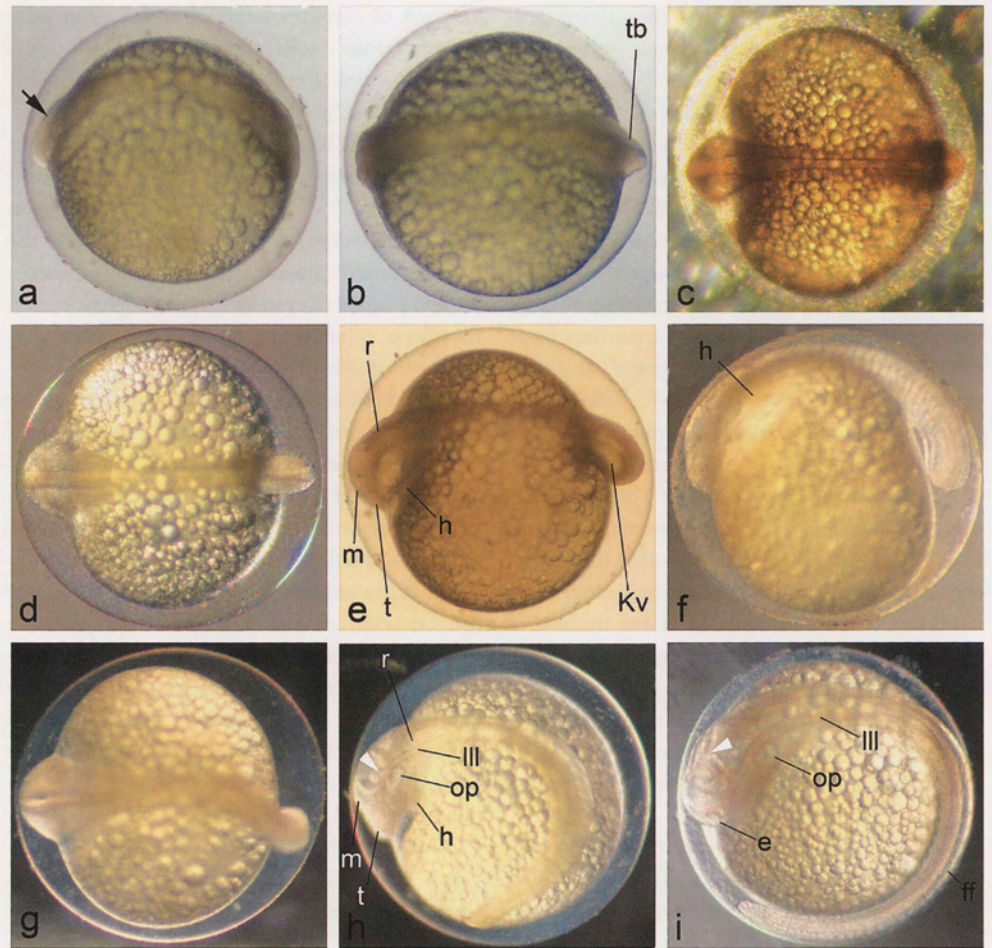
**Stage 23/heartbeat stage:** Apart from first contractions of the heart and the presence of a few red blood cells, this stage is characterized by a 90° bend of the free trunk-tail (fig. 5 f, 35:11). The somites and the mesoderm destined for the further differentiation of somites is fused at the midline above the spinal cord, and the mesodermal matter of the lateral plates in the head region grows dorsally, too. The embryo protrudes the epidermal yolk sac cover and is laterally compressed, except in the head region. The embryo now has 19-20 somites. The earliest somatic muscular activity occurs in the posterior trunk-tail region. The observed contractions were mostly weak lateral trunk-tail flexions. Touching the embryo will first elicit a single twitch, then later a secondary backlash or even several thrashes of the tail.

**Stage 24/fin fold stage:** First sign of the embryonic fin fold is discerned, but it has a very low profile, still (fig. 5 g). It runs along the midline from the first somite caudally and

---

beherbergt dicht gepackte Vakuolen; c Stadium 13, 50% Epibolie-Stadium, Neuralplattenbildung; die Region des Blastoderms, wo der Embryonalschild (es) lokalisiert ist, scheint weiter vegetad gewandert zu sein als das übrige Blastoderm; die Vakuolen befinden sich direkt hinter dem Keimring (gr) und folgen der epibolischen Bewegung; d Stadium 14, 75% Epibolie-Stadium mit Beginn der Neurulation; der Dotterpfropf (yp) ist begrenzt von einem flachen und kurzen Keimring (gr); beachte die hohe Konzentration der Vakuolen um die Neuralplatte herum (npl), Dotter unterhalb der Evakuationszone eingedrückt; e Stadium 15, Stadium mit keilartiger Neuralplatte, differenziert in prospektive Gehirn- (weißer Pfeil) und Rumpfbzone (schwarzer Pfeil); f Stadium 16, Embryo, Epibolie beendet bei gleichzeitigem Auftreten der ersten drei Somiten (som) und Präsenz der anterioren primären Dotterhöhle/Perikardialhöhle unterhalb der Gehirnregion (weißer Pfeil); Stadium 17 (g, h), g beachte den Rest der Evakuationszone (weißer Pfeil), die Dotterhöhle (yc) unterhalb der gesamten Neuralplatte und bei h eine Dorsalansicht des Keimes von (g), der die löffelfartige, in der Mittellinie gelegene Region der Neuralplatte mit der Chorda (schwarzer Pfeil) zeigt. bp – Blastoporus, dbp – Blastoporuslippe. Skala: 1 mm.





**Figs. 5 a-i:** Neurulation (a-c) and subsequent organogenesis (d-i) in *Pollimyrus isidori*. **a** Stage 18, dumbbell-shaped neural plate with elevated anterior neural folds (arrow) and closed blastopore; **b** stage 19, early trunk-tail bud (tb); the large neural groove becomes evident along the midline of the plate, with a still widened depression at the anterior end; **c** stage 20, club-shaped embryo; note the establishment of the neural keel and the constriction between prosencephalon and deutencephalon; **d** stage 21, neural rod/tube stage, final process of neurulation by fusion of the neural folds in the midline in the anterior body region; **e** stage 22, tail bud bent; Kupffer's vesicle (Kv) appears in the bent tail bud; **f** stage 23, heartbeats observed; 90° tail-bud bend; first trunk-tail contractions; **g** stage 24, fin fold stage, note the undulatory shape of the trunk-tail during movement; **h** stage 25; note the enlargement of the head caused by further brain differentiation; arrowhead points to the corpus cerebelli; **i** stage 26, „C“-shaped pre-hatching embryo. ff—fin fold, e—eye, h—heart, Ill—lobi lineae lateralis, m—mesencephalon, op—otic placode, r—rhombencephalon, t—telencephalon. Scale bar: 1 mm.

**Abb. 5 a-i:** Neurulation (a-c) und nachfolgend Organogenese (d-i) bei *Pollimyrus isidori*. **a** Stadium 18, Neuralplatte mit aufgewölbten vorderen Neuralfalten (Pfeil) und geschlossenem Blastoporus; **b** Stadium 19, frühes Schwanzknospenstadium (tb); die große Neuralfalte wird sichtbar in der Mittellinie der Neuralplatte mit einer geweiteten Absenkung am anterioren Ende; **c** Stadium 20, knüppelartiger Embryo; beachte die Herausbildung der Neuralkuppe und die Einschnürung zwischen Prosencephalon und Deutencephalon; **d** Stadium 21, Neuralrohr Stadium; finaler Prozess der Neurulation durch Fusion der Neuralfalten in der



encircles the entire trunk-tail end. Thrashing movements become a constant activity of the trunk and tail region. There are 23-24 somites visible now. A dorsal aorta is visible in the anterior body region. At the ventro-posterior yolk surface the primordial subintestinal and vitelline veins are established.

**Stage 25/otic placode:** The entire head region has enlarged quickly, and shows several changes and new features (fig. 5 h, 51:13). Adjacent to the fissura rhombo-mesencephalica, posteriorly, the corpus cerebelli forms first as two, paired conspicuous columns. The oblique walls of the rhombencephalon, the lobi lineae lateralis (lll), become visible. The telencephalon appears as a narrow projection forward from the mesencephalic area. The otic placode emerges for the first time. The yolk sac is covered by a dense plexus of anastomosing subintestinal venae vitellinae. Spontaneous vigorous flexion movements of the body are common, which cause the embryo to rotate within the chorion. If illumination is changed, contraction frequency is temporarily increased. The membranous embryonic fin fold becomes conspicuous.

**Stage 26/pre-hatching stage:** In immobile condition the tip of the curved trunk-tail region reaches the vertical of the head end (fig. 5 i, 62:09). This tip touches or passes over the head during movements. The yolk cavity is enlarged beyond the entire anterior part of the embryo still attached to the epidermal yolk sac cover. The anterior part of the head is slightly undercut at its juncture with the epidermal yolk sac cover (first indication of the head lift). The elliptic otic placode has enlarged and invaginates into an otic vesicle in which two first condensations of otoliths are discerned as small black spots. A lens is formed inside the eye cup, when the choroid fissure is still wide open. The mus-

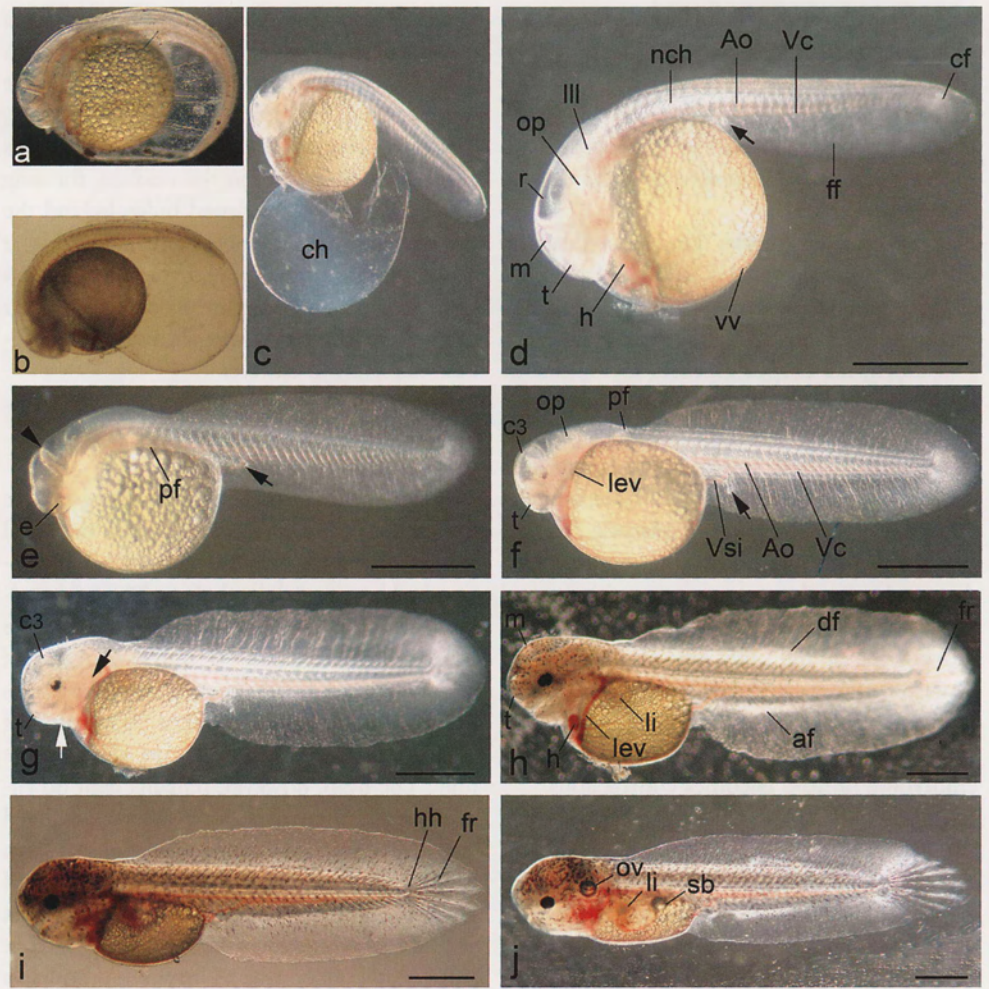
cular contractions of the embryo now are powerful movements of the entire body. These movements are sufficient to change orientation of the embryo inside the chorion. The two columns of the presumptive corpus cerebelli fuse dorsally in the midline, forming also a transversally widened bulge behind the fissura rhombo-mesencephalica. This bulge curves forward, inwards and ventrally and also grows caudally, forming the primitive cerebellar cavity. The lobi lineae lateralis are very prominent and start to elevate.

### 3.1.2. Free embryonic phase

**Stage 27/hatching stage:** Hatching is rare before this stage. Hatching in mass occurred around seventy hours after spawning. The chorion had lost its stability before. The tail usually protrudes first (fig. 6 a) and then the whole embryo liberates (fig. 6 b). After the rupture of the chorion the free embryo often still remains within the chorion for some time. After hatching straightening of the body occurs after a short time. The head, however, remains bent downwards along the yolk sphere; the axes of head and body meet at an angle of about 90° (figs. 6 c, d, 68:00). When stimulated, the hatched embryo performs repeated lashes of its trunk and tail, but merely whirls around in circles. Apparently, early free embryos are still too heavy for directed movements. The mouth and anus are not yet open. No pigment is discernible, even not in the eye. A mesenchyme concentration can be seen in the translucent median ventral fin fold beyond the upward flexed notochord end. This is the anlage of the caudal fin. A thickening of tissues in the ventral fin fold below somites 9-12 indicates the development of the primary gut canal. There have

Mittellinie in der vorderen Körperregion; e Stadium 22, Schwanzknospenkrümmung; Kupffer'scher Vesikel (Kv) erscheint in der gebogenen Schwanzknospe; f Stadium 23, Beginn des Herzschlags; Schwanzknospenkrümmung 90°; erste Rumpf-Schwanz-Kontraktionen; g Stadium 24, Flossensaum-Stadium; beachte die Biegung des Rumpf-Schwanzes während der Bewegung; h Stadium 25; beachte die Vergrößerung des Kopfes bedingt durch eine weitere Gehirndifferenzierung; Pfeilspitze zeigt auf den corpus cerebelli; i Stadium 26, „C“-gestalteter Embryo vor dem Schlupf. ff – Flossensaum, e – Auge, h – Herz, lll – lobi lineae lateralis. m – Mesencephalon, op – Ohr-Placode, r – Rhombencephalon, t – Telencephalon. Skala: 1 mm.





**Figs. 6 a-j:** Hatching process (a-c) and free embryonic development (d-j) of *Pollimyrus isidori*. **a** Embryo straightening inside the weak chorion, indicating enzymatic lysis; **b** rupture of the chorion and free anterior part of the embryo; **c** stage 27, free embryo, just hatched, still attached to the remnant of the chorion; **d** specimen of (c) magnified; note the descend of the heart (h) into the enlarged pericardial cavity and presence of the caudal fin mesenchyme (cf) concentration; **e** stage 28, pectoral fin bud (pf); **f** stage 29, first eye pigment and rectal tube bent; note the developed fin fold capillary network; **g** stage 30, establishment of the jaw and branchial arch placodes (white and black arrows, respectively); **h** stage 31, dorsal and anal fin anlage (df, af, respectively) with mesenchymatous buds and differentiation of the first caudal fin ray (fr) primordia; **i** stage 32, mouth opening stage with notched caudal fin and haemal and hypural plate (hh) distinct; **j** stage 33, primordium of swim bladder (sb) and gas-filled otic vesicle (ov) can be distinguished; note the borderline at the transition between the caudal fin and fin fold. Ao – aorta dorsalis, c3 – central lobe of cerebellum, e – eye, ff – fin fold, lev – left efferent vena vitellina, li – liver, III – lobi lineae lateralis, m – mesencephalon, nch – notochord, op – otic placode, r – rhombencephalon, t – telencephalon, Vc – vena caudalis, Vsi – vena subintestinalis, vv – venae vitellinae; arrows point to the rectal tube except in (g). Scale bars: 1 mm.

**Abb. 6 a-j:** Schlüpfvorgang (a-c) und Entwicklung des freien Embryos (d-j) von *Pollimyrus isidori*. **a** Embryo-Streckung innerhalb des weichen Chorions, dies vermutlich verursacht durch enzymatische Lysis; **b** Zerreißen des Chorions und freier, vorderer Teil des Embryos; **c** Stadium 27, freier Embryo, soeben geschlüpft, noch angeheftet an den Resten des Chorions; **d** Embryo von (c) vergrößert; beachte die Absen-



been evident changes in the outer appearance and structure of the head. The head process has already undergone a significant lift. Several structures are better defined. In particular, the heart is beginning to descend into the pericardial cavity. The excavation of the yolk sac cavity continues ventro-laterally and exposes the heart with the associate arterial and venous vessels. The straightening of the embryo now allows to follow the blood circulation in more detail. The red blood cells circulate through a simple system that includes: A two-chambered heart with a central atrio-ventricular constriction; a ventral aorta running forward underneath the head with indistinct branched branchial arteries; a dorsal aorta, from the head region to the end of the trunk-tail region; a vena caudalis, and finally, a diffuse and apparently random course of a vitelline vein system across the external ventral surface of the yolk mass, back to the heart. An eye-catching blood vessel between the corpus cerebelli and the mesencephalon is visible, possibly the ophthalmic and major cerebral artery, but its origin and destination cannot be followed by external inspection. All myomeres receive blood from the segmental vessels. There are 32 to 34 pairs of somites and all except the hindmost and least differentiated display a slightly arched shape, convex anteriorly.

**Stage 28/pectoral fin bud:** There is a rather sudden emergence of the pectoral fin buds. This tiny, semicircular pectoral fin projects from the dorsal epidermal yolk sac cover, and stands vertical in a parasagittal plane to the embryo.

The upwards flexion of the end of the notochord has reached its final shape perpendicular to the longitudinal axis of the embryo (fig. 6 e, 86:11) and a high dorsal median fin fold is fully formed. The lobi lineae lateralis of the rhombencephalon are elevated to fuse in the midline, as the adjacent transversal bulge of the corpus cerebelli becomes conspicuous. The subintestinal venae vitellinae run around the right side of the robust rectal canal. A capillary network of the fin fold establishes, but the capillaries do not reach the most peripheral region of the fin fold.

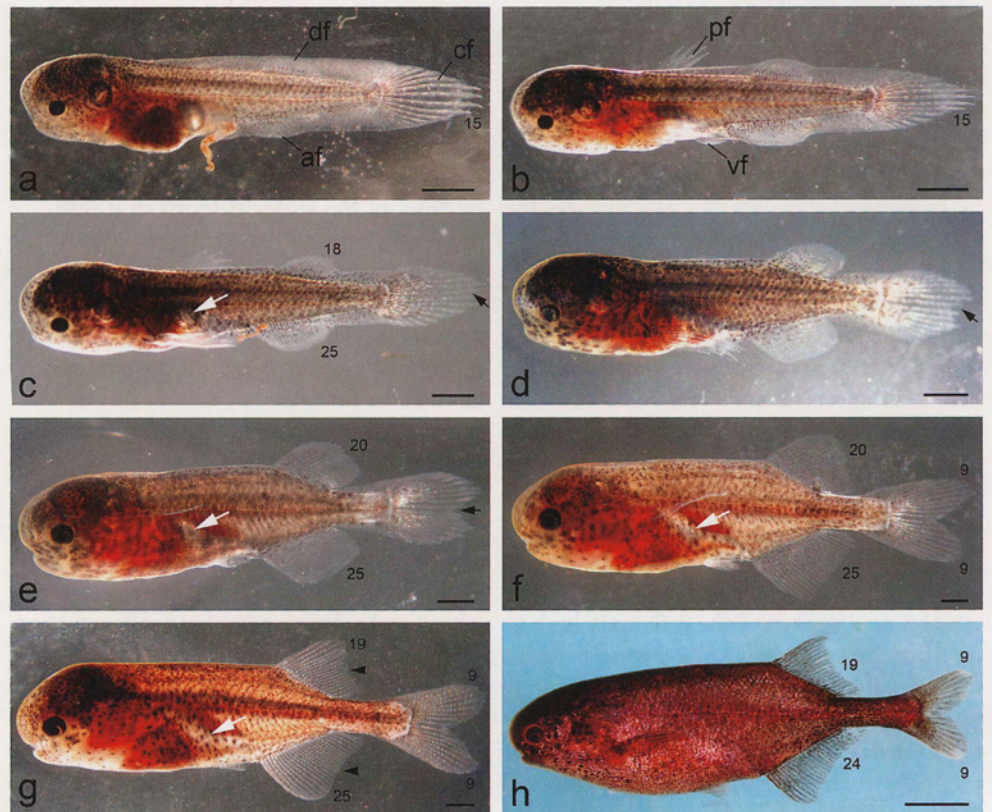
**Stage 29/eye pigment:** The pectoral fin bud differentiates into a broadened proximal peduncle and a thin peripheral area (fig. 6 f, 4 days). The rectal tube bends ventrally. The continued lift of the head from the yolk sphere exposes the stomodeal plate. Usually the yolk mass is no longer rounded, but has become egg-shaped, narrow at its posterior end. Diffuse pigment appears in the eye. A few small unbranched melanophores that contain diffuse melanine pigment are distributed all over the ectoderm of the head. Mesodermal mesenchyme concentrates around the otic plate. The first typically mormyrid cerebellar structure starts to develop. The central lobe C3 becomes clearly visible. The vascular fin fold network extends now over the entire fin fold area. Some larger venae vitellinae are established at the lateral region of the yolk mass surface.

**Stage 30/jaw and branchial placode:** The first mesenchymal condensations of jaws and branchial arches can be seen between head and

---

kung des Herzens (h) in die vergrößerte Perikardialhöhle hinein und die Präsenz des Schwanzflossen-Mesenchyms (cf); e Stadium 28, Brustflossenknospe (pf); f Stadium 29, erstes Augenpigment und abgebo-  
genes Enddarmrohr; beachte das entwickelte kapillare Netzwerk des Flossensaumes; g Stadium 30, Ausbil-  
dung von Kiefer- und Kiemenbogenplakoden (weiße und schwarze Pfeile); h Stadium 31, Anlage von  
Rücken- und Afterflosse (df, af) mit mesenchymatischen Knospen und Differenzierung der ersten Primor-  
dien der Schwanzflossenstrahlen (fr); i Stadium 32, Stadium der Mundöffnung mit eingekerbter Schwanz-  
flosse und distinkten Haemalfortsätzen und hypuralen Platten (hh); j Stadium 33, Schwimmblasen-Primor-  
dium (sb) und gasgefüllter Ohrvesikel (ov) sind sichtbar; beachte die Grenzlinie am Übergang zwischen der  
Schwanzflosse und dem Flossensaum; Ao – Aorta dorsalis, c3 – zentraler Lobus des Cerebellums, e – Auge,  
ff – Flossensaum, lev – linke efferente vena vitellina, li – Leber, ll – lobi lineae lateralis, m – Mesencepha-  
lon, nch – Chorda, op – Ohr-Placode, r – Rhombencephalon, t – Telencephalon, Vc – vena caudalis, Vsi –  
vena subintestinalis, vv – venae vitellinae; Pfeile zeigen auf den Enddarmtubus außer in (g). Skala: 1 mm.





**Figs. 7 a-h:** Larval development of *Pollimyrus isidori*. **a** Stage 34, onset of exogenous feeding coinciding with the formation of primordial rays in the dorsal and anal fins (df, af, respectively); **b** stage 35, note the presence of the ventral fin bud (vf), the fully developed pectoral fin (pf); **c** stage 36, pronounced regression of the median fin fold; **d** stage 37, haemal and hypural processes become covered by muscles; **e** stage 38; note the trapezoidal appearance of dorsal and anal fins and the indentation of the caudal lobe (arrow); **f** stage 39, clearly bilobate and slightly heterocercal caudalis, almost triangular dorsal and anal fins, median fin fold has almost vanished; **g** stage 40, juvenile; note the concave trailing edge of the dorsal and anal fin (black arrow heads); **h** adult female (7.3 cm total length). Black numbers concern the numbers of finrays. Black arrow indicates the borderline between dorsal and ventral lobes of the caudal fin, and white arrows point to the swim bladder. Scale bar: 1 mm.

**Abb. 7 a-h:** Larval-Entwicklung von *Pollimyrus isidori*. **a** Stadium 34, Beginn der exogenen Nahrungsaufnahme bei gleichzeitiger Bildung der primordialen Flossenstrahlen in Rücken- und Afterflosse (df, af); **b** Stadium 35; beachte die Präsenz der Bauchflossenknospe (vf) und die vollständig entwickelten Brustflossen (pf); **c** Stadium 36, starke Rückbildung des embryonalen Flossensaumes; **d** Stadium 37, Haemal- und Hypuralfortsätze werden von Muskeln überdeckt; **e** Stadium 38; beachte die trapezartige Form von Dorsal- und Analflosse und die Einbuchtung der Schwanzflosse (Pfeil); **f** Stadium 39, eindeutig zweilappige und leicht heterocercal Caudalis, fast dreieckige Dorsal- und Analflossen, embryonaler Flossensaum fast vollständig resorbiert; **g** Stadium 40, juveniler Fisch; beachte die Einbuchtung bei Dorsal- und Analflosse (schwarze Pfeilspitzen); **h** adultes Weibchen (7.3 cm Gesamtlänge). Schwarze Zahlen geben Flossenstrahlzahlen an. Schwarze Pfeile zeigen die Grenze zwischen oberem und unterem Lobus der Caudalflosse an, weiße Pfeile die Schwimmblase. Skala: 1 mm.



**Tab. 1:** Overview of the early developmental stages of *Pollimyrus isidori*. The characters without parentheses correspond to defining criteria and those in parentheses to concurrent features.

**Tab. 1:** Übersichtstafel der frühen Entwicklungsstadien von *Pollimyrus isidori*. Benannt sind die stadiendefinierenden Kriterien. In Klammern gesetzt sind "begleitende" – spezifische Merkmale der Art oder Familie.

Stage No	Short term of stage	Defining criteria (some major concurrent features)
Embryonic period: embryonic or "chorioned" phase		
1	1-cell	formation of the perivitelline space and the blastodisc
2	2-cell	first meridional cleavage
3	4-cell	second cleavage perpendicular to the first one
4	8-cell	two synchronous cleavages perpendicular to the second one, on either side of the first one
5	morula / 9 to 32-cell	onset of asynchronous cleavage and yolk syncytial layer (blastodisc dome shaped, juncture between blastodisc and yolk groove-like)
6	early blastula	enveloping layer (Evl) and deep layer cells (Dc) form
7	high blastula	Dc in multilayered condition (blastoderm opaque, the marginal Dc is irregular in shape)
8	flat blastula	phase I of epiboly, flattening of the blastoderm by migration of Dc vegetally (Evl smooth)
9	late blastula	blastoderm lens-shaped and translucent of almost uniform thickness, surface of yolk flat
10	onset epiboly proper	blastoderm starts to spread vegetally (yolk bulges towards animal pole, blastoderm translucent, around 15% yolk coverage)
11	embryonic shield	germ ring and embryonic shield form (Dc of the central blastoderm migrates, 20% yolk coverage)
12	evacuation zone	Dc leaves central area of the blastoderm (30% yolk coverage,)
13	extension / culumination	columnarisation of the ectodermal epithelium to form a neural plate and clear appearance of the germ ring (only Evl roofs evacuation zone (ez), 50% yolk coverage)
14	neural plate	neural plate formation (yolk plug forms, 75% yolk coverage, evacuation zone hollowed out to larger extent)
15	wedge-shaped neural plate	wedge-shaped neural plate (brain region represents $\frac{2}{3}$ of the neural plate, 90% yolk coverage)
16	onset somatogenesis	first somites appear (brain region represents almost $\frac{1}{2}$ of the neural plate length)
17	end-epiboly	yolk completely wrapped by the blastoderm (blastopore still open)
18	dumbbell-shape	blastopore closed and concentration of the prospective tail bud mesodermal material
19	early tail bud	tail-bud formed, neural plate started to infold at the midline caudally
20	brain regionalization	brain differentiates into pros- and rhombencephalon
21	neural rod	neural folds fuse into a cylindrical neural rod or tube
22	heart tube	emergence of heart and Kupffer's vesicle (3 brain vesicles recognized: tel-, mes-, and rhombencephalic region; tail bud bent)
23	heartbeat	heart beats and somites grown over the neural rod (tail 90° bend, wide pericardial cavity)
24	fin fold	fin fold forms, appearance of medioventral vena vitellina (thrashing movements in the trunk)
25	otic placode	otic placode visible; fissura rhombo-mesencephalica (corpus cerebelli, lobus lineae lateralis)
26	pre-hatching	eye cup and bulged lens, corpus cerebelli fused dorsally (rostral undercutting of head process)
Embryonic period: free embryonic phase		
27	hatching	free embryo club-shaped, caudal fin mesenchyme (notochord flexion)
28	pectoral fin bud	pectoral fin bud, corpus cerebelli as a transversal bulge (fin fold capillary network)
29	eye pigment	first eye and head pigment (conspicuous fin fold capillary network, rectal tube bent)
30	jaw and branchial placodes	jaw and branchial placodes
31	dorsal and anal fin buds	dorsal and anal fin mesenchyme, caudal fin rays primordia (lower and upper jaw forms, liver)
32	mouth opening	mouth open, pectoral and caudal fins notched
33	swim bladder and otic vesicle	swim bladder and otic vesicle appear



Tab. 1: Continued.

Tab. 1: Fortsetzung.

Larval period: finfold larva		
34	onset feeding	first exogenous feeding, primordial rays formed in dorsal and anal fins
35	ventral fin bud	ventral fin buds (pectoral fin fully developed and functional)
36	unpaired fins demarcation	unpaired fins demarcated from the fin fold, haemal and hypural processes covered by muscles (ray complement in developed anal and dorsal fins)
37	caudal lobes separation	borderline dorsal-anal lobe of caudal fin (dorsal and anal fins separated from the peduncle fin fold)
38	Swim bladder elongation	Swim bladder elongates to connect with the otic organ (dorsal and anal fins trapezoidal)
Larval period: finformed larva		
39	pelvic fin	pelvic fins formed, complete regression of the fin fold (homocercal caudal fin, dorsal and anal fins triangular)
40	juvenile	completion of squamation, shape of fins similar to the adult.

yolk mass (fig. 6 g, 5 days). The pectoral fin bud becomes ellipsoid in shape by dorsocaudal prolongation. Its rostral edge approaches the body, while the caudal edge sticks out from the body. The first vessel loop appears parallel to the rim of the peduncle. The central lobe of the corpus cerebelli C3 and the telencephalon still form the most rostral part of the free embryo. The pharynx can be clearly seen through the transparent embryo. There are four areas of mesenchyme seen in the caudal median fin fold, the mesodermal and ectodermal anlagen of the future hypurals and caudal fin rays, respectively. The greatly reduced yolk sac has a "streamlined" egg shape now. Accordingly, proportionally more yolk is exposed to the vitelline vascular resorption system.

**Stage 31/dorsal and anal fin buds:** The anlagen of the dorsal and anal fins appear simultaneously as denser concentrations of mesenchyme in the fin fold (fig. 6 h, 6 days). The formation of the first rays in the caudal fin is distinct now. The pectoral fin anlage becomes circular with an enlarged and indented rim. Its insertion base is obliquely positioned antero-dorsally. The telencephalon extends rostrally and becomes the anteriormost part of the brain. Further head lift and regression of the yolk, combined with the growth and straightening of the head exposes the underside of the head and the future mouth opening as a ">"-shaped separation between upper and lower jaws, the two-chambered heart, and first branchial arches. The liver is visible in the dorsal yolk mass. Me-

lanophores with branched arms increase in number in the head region, and they appear for the first time also on the trunk and tail. A vascular network of the caudal fin is established. The network of vitelline veins is denser, mainly caused by the reduction of yolk volume.

**Stage 32/mouth opening:** The number of rays in the caudal fin has increased to 8 (fig. 6 i, 7 days). They have remarkably extended, reaching also the border of the fin fold, which becomes notched. The haemal and hypural processes become visible. Head lift is almost complete. Further opening of the stomodeal plate exposes the small, immobile gape of the mouth. The eyes are entirely black. Pectoral fins are well developed, with a vertical base and they are mobile. The olfactory placode, with a central depression, becomes visible rostral to the eye. The density of melanophores increases in the dorsal epidermis overlying and obscuring the inner detail of the head. The melanophores have multiplied in the trunk and tail, and also dispersed into the proximal areas of the fin fold and the caudal fin. The opercular flap and opening start to form at the anterior margin of the yolk sac.

**Stage 33/swim bladder and otic vesicle:** A small amount of gas appears simultaneously in the swim bladder anlage and otic vesicles (fig. 6 j, 10 days). The caudal fin is demarcated from the fin fold by the regression of the latter at its posterior end. The central lepidotrichial rays start to segment. The lower jaw is completely free from the yolk sac and has elongated and



straightened, but still the mouth cannot be closed. Four branchial arches can be made out behind the eye and above the heart. Only a thin layer of yolk separates the stomach from the ventral epidermal yolk sac cover.

### 3.2. Larval period

**Stage 34/onset of feeding:** This first stage of the larval period is characterized by exogenous feeding concurrent with endogenous nutrient-utilization (fig. 7 a, 14 days). Yolk is reduced to a tiny remnant. At the beginning of first feeding the larvae show little mobility, remain at the same place on the bottom of the dish, and seize the prey that is passing close by. Development of the opercular membrane and slit have also proceeded and the opercular folds are attached to the gular region far cranially alone, which results in the openings reaching far cranially to the isthmus region, too. In this stage active breathing movements by rhythmic buccal expansions and movements of the gill cover are first observed. The mouth also opens and closes rhythmically. The lower fin fold presents a slight convex projection at the dorsal and anal fin. Internally in both the dorsal and anal fins 14-15 and 16-18 rays are differentiated, respectively, but they are not yet segmented. The caudal fin has become pointed, and consists of 15 segmented rays. 34 myomeres are present. This is the highest number of myomeres observed in the larva and should correspond well to the juvenile and adult myomere number (adult vertebral count is 37). Melanophores become abundant in all the exposed ectoderm of the early larva and their high density of melanin more and more obscures the inner detail of the head.

**Stage 35/ventral fin bud:** The dorsal and anal fins extend over the embryonic fin fold (fig. 7 b, 17 days). Just anterior to the anal fin, the anlage of the ventral/pelvic fin is formed first as a membranous bud. The caudal fin still remains pointed. The pectoral fins are fully formed with 6 segmented lepidotrichial rays each, and are fully functional too, and are used for maneuvering and propulsion by the larva.

Their bases are almost at a right angle to the body axis. Melanophores blacken the dorsal head surface. Nostrils are clearly observed. The larvae start to swim actively, though their ability to maneuver is very limited still. From time to time, they stop swimming and sink to the bottom.

**Stage 36/unpaired fin demarcation:** The continued regression of the median fin fold permits to determine the contour of the dorsal, anal, and caudal fins (fig. 7 c, 20 days). The haemal and hypural processes are covered by muscles. From this stage onward, the mobility increases, and active hunting or search for higher food densities is performed. The larvae show a certain aggression and often the pectoral fins are bitten off. The fins apparently are very sensible to damage and will hardly regenerate after injury. Such injuries were found to be a major factor of larval mortality, because often infections by bacteria, histophagous ciliates and fungi resulted.

**Stage 37/caudal lobe separation:** The dorsal and anal fins separate from the peduncular fin fold remnant and the asymmetry of the caudal fin has become more conspicuous (fig. 7 d, 23 days). The caudal fin exhibits at first an asymmetric shape indicating the onset of the separation between its upper and lower lobes. The larvae attain a rather high body, but the head still remains higher.

**Stage 38/swim bladder elongation:** The homocercal, bifurcate caudal fin starts to form (fig. 7 e, 31 days). Each lobe consists of 9 rays. 20 and 25 rays, partly segmented, were counted in the dorsal and anal fins, respectively. The dorsal and anal fins assume a trapezoidal-shape. The swim bladder starts to elongate dorso-rostrally to connect with the otic vesicle. There is an obvious change in the pigmentation pattern at the transition from the larval to the juvenile period.

**Stage 39/pelvic fin:** The pelvic fins, which are the last to form, have fully differentiated and are mobile (fig. 7 f, 45 days). The dorsal and anal fins lose their trapezoidal shape, become fully developed in size and the triangular adult shape is reached. The fin fold of the cau-



dal peduncle has regressed completely. Intra-specific aggressiveness markedly decreases. The specimens have attained the general body profile of the juvenile form now.

**Stage 40/juvenile:** The maximum head depth is almost the same as that of the body. In both, dorsal and anal fins a shallow depression appears at the distal edges, similar to the definitive adult shape (fig. 7 g, 50 days). The final shape of the tail is reached by the conspicuous constriction and complete regression of the remaining fin fold at the caudal end of the peduncle. However, the head shape and pigmentation pattern are still different to those of the adult (fig. 7 h).

#### 4. Discussion

Published documentation on reproductive style and behaviour, egg, embryo, and larval characters of Osteoglossomorpha were summarized by BREDER & ROSEN (1966) and recently by BRITZ (2004) and by KIRSCHBAUM & SCHUGARDT (2002a, 2006) for mormyrids. No osteoglossomorph species has been studied in sufficient detail and completeness to identify basic unique developmental patterns within the group. Most published descriptions are non-sequential, characterizing hatching embryos and early larvae on the basis of a few typical specimens. In contrast, our study on *Pollimyrus isidori* represents the first detailed description of development. We thus were also able to propose for the first time a staging system for an osteoglossomorph fish.

##### 4.1 Egg and reproductive style

Eggs of *Pollimyrus isidori* like those of *Marcusenius mento* (Boulenger, 1890) and *Campylomormyrus tamandua* (Günther, 1864) measure 2 mm in diameter (KIRSCHBAUM & SCHUGARDT 2006). This is larger than egg size of *Petrocephalus soudanensis* (Bigorne & Paugy, 1991), but smaller than the egg size of *Pollimyrus adspersus* (Günther, 1866). The chorion of *P. isidori* and *P. adspersus* is non-adhesive. These are the only two mormyrid species which are known to show

parental care. The nesting and guarding of the eggs and young is restricted to the male. Elements of reproductive strategy and descriptions of courtship documented for *P. adspersus* (CRAWFORD et al. 1986, KIRSCHBAUM 1987) are similar to that observed in *P. isidori*. Eggs of other mormyrids that show no nesting and parental care activities, like *Hippopotamyrus pictus* (Marcusenius, 1864), *Campylomormyrus tamandua* (Günther, 1864), *Campylomormyrus* sp., and *Mormyrus rume probosciostris* (Boulenger, 1898), were slightly to strongly adhesive for some limited time after spawning (KIRSCHBAUM & SCHUGARDT 2002a). Adhesiveness is interpreted to have adaptive significance for certain ecological functions: avoidance of drift from the spawning habitat and keeping the eggs in well oxygenated areas (e.g. RIEHL 1996, BARTSCH et al. 1997).

The two species of Hiodontidae, *Hiodon alosoides* (BATTLE & SPRULES 1960) and *H. tergisus* (SNYDER & DOUGLAS 1978), and the single representative *Pantodon buchholzi* (MOHN 1976 a, b, BRITZ 2004) of the family Pantodontidae exhibit no parental care. Eggs of *P. buchholzi* are spherical with a transparent chorion and measure about 2 mm (MOHN 1976 a) and 2.2–2.4 mm (BRITZ 2004) in diameter, respectively, and they float at the water surface. This buoyancy is due to several, usually 5–7 large oil globules above the yolk (BRITZ 2004). The semi-transparent and spherical eggs of *Hiodon alosoides* (BATTLE & SPRULES 1960) and the oval eggs of *H. tergisus* possess a single large oil globule, are free-floating at some depth and may be referred to as semi-buoyant or semi-pelagic. Newly hatched free embryos of *H. alosoides* float in a vertical position at the water surface the head upwards, probable because of the buoyant effect of the oil globule (BATTLE & SPRULES 1960). Such a floating in vertical position was observed also in early free embryos of *P. isidori*, but for quite different reason: in these, for some time it may occur when the swim bladder vesicle becomes conspicuous occupying the entire region behind the stomach.

In species of the genera *Scleropages* and *Osteoglossum*, large eggs (10–19 mm, see BRITZ



2004, RIEHL personal communication) are carried by the male and/or female in the mouth. Besides, *Heterotis niloticus* (BUDGETT 1901) and *Arapaima gigas* (LÜLING 1964, 1969) build nests and guard their eggs and young. In *H. niloticus* the eggs sink to the bottom of the nest where they adhere to each other forming a large egg mass. In Notopteridae, in the species of the genera *Notopterus* and *Chitala*, eggs are attached to the substrate and eggs and young are guarded by the male or by both parents (see BRITZ 2004).

The surface of the spawned egg of *P. isidori* appears smooth at binocular magnifications, but a lower, curly microplicae net, which covers the entire surface of the chorion and shows agglutination and stretched appearance of some of these microplicae, is detected by scanning electron microscopy. The chorion of *Pantodon buchholzi* (BRITZ 2004) is also smooth when observed at binocular magnifications. In SEM preparations it shows numerous and regularly structured pores that can be found in many freshwater teleostean eggs as in *Alosa pseudoharengus* (JOHSON & WERNER 1986), *Piaractus mesopotamicus*, *Serrasalmus spilopleura* (RIZZO et al. 2002), for example. The semi-transparent chorion of *Hiodon alosoides* described by BATTLE & SPRULES (1960) also shows small pores or depressions located at the tip of regularly spaced elevations.

#### 4.2 Embryonic and larval development

The earliest development up to the blastula stage as defined by stages 1-10 of *P. isidori* (representative for mormyrids) bears general resemblance to the osteoglossomorphs *Pantodon buchholzi* (BRITZ 2004) and *Hiodon alosoides* (BATTLE & SPRULES, 1960), but also to more distantly related taxa like clupeids as represented by Shad, *Alosa sapidissima* (SHADO 1995), to cyprinids as demonstrated in the Rosy barb *Barbus conchoni* (WOOD & TIMMERMAN 1988, GEVERS & TIMMERMAN 1991) even to percormorphs as represented e.g. by *Cichlasoma dimerus* (MEIJIDE & GUERRERO 2000) and *Stizostedion vitreum* (= *Sander vitreus* (Mitchill, 1818)) (MCELMAN & BALON 1979).

Shortly after spawning, a small region of free-yolk cytoplasm at the animal cap of the egg forms, followed by meridional cleavage of the blastodisc into numerous blastomeres. As in most of the cases of meroblastic cleavage, the first cleavage furrows occur synchronously at regular orientations. However, also some variation in the cleavage pattern exists among teleosts. In *P. isidori* regular orientation and synchronicity in the timing of the cleavage furrows is lost in the fourth cleavage circle after formation of eight blastomeres. This may happen in other teleosts considerably later, at the seventh set of cleavages after 64-blastomeres in the cyprinid zebrafish *Danio rerio*, for example (KIMMEL et al. 1995). The blastulation in *P. isidori* does not involve blastocoel formation, but rather tiny intercellular spaces exist between the deep cells of the blastoderm. KIMMEL et al. (1995) have mentioned that the term "Stereo-blastula" would be more appropriate than blastula to describe this condition and interval of ontogeny in teleosts, for it means no true uniform cavity or blastocoel is present.

The yolk syncytial layer (Ysl) may be extraembryonic, making no direct contribution to the body of the embryo. The Ysl has the role of directing the cell movements which establish the embryonic shield during normal morphogenesis (LONG 2005). "At first the Ysl has the form of a narrow ring of yolk syncytial nuclei around the blastodisc edge but soon some Ysl nuclei (Ysn) spread underneath the blastodisc, forming a complete "internal" syncytium (the i-Ysl), that persists throughout embryogenesis. In this position, between the embryonic cells and their yolk stores, the i-Ysl is presumed to be playing a nutritive role" (KIMMEL et al. 1995, p. 265). Another portion of the Ysl moves vegetally, staying ahead of the blastoderm margin, to form the external Ysl (e-Ysl). Indeed, work on the teleost *Fundulus heteroclitus* shows that the e-Ysl appears to be a major motor for epiboly (TRINKAUS 1984). In *Danio rerio* (KIMMEL & LAW 1985) the Ysl forms at the time of the 10<sup>th</sup> (sometimes the 9<sup>th</sup>) cleavage when the cells at the vegetal edge of the blastoderm fuse with the underlying yolk cell. For the



formation of the Ysl in *F. heteroclitus* TRINKAUS (1993) states that, as in other teleosts, the *F. heteroclitus* Ysl forms mainly by collapse of certain marginal blastomeres which then merge with the cytoplasm of the yolk cell peripheral to the blastoderm. Nuclei enter the yolk cell from these open blastomeres variably during cleavages 8-11, but most frequently at cleavages 9 and 10. The establishment of the Ysl in *P. isidori* seems similar in this respect to *Danio rerio*, but occurs earlier at the 4<sup>th</sup> cleavage set (stage 5) when the cleavage furrows become asynchronous.

The first ontogenetic cell movement in meroblastic teleosts is the epiboly of the blastoderm cells over the yolk. The Ysl is considered to be the source of the control of cell movements by contact guidance during epiboly and convergence (LONG 1984). Mechanisms of epiboly and the mode of movement of the deep cells were described and experimentally studied mainly in *Danio rerio* (TRINKAUS 1984, 1992), and in *F. heteroclitus* (TRINKAUS & LENTZ 1967, TRINKAUS & ERICKSON 1983). During phase I epiboly also in *P. isidori* there is a general migration of the deep cells away from the animal pole toward the margin of the blastoderm, thinning the blastoderm area centrally and thickening it at the periphery. In phase II epiboly migration of deep cells continues from the animal pole, between the enveloping cell layer and the Ysl. So far, all descriptions of teleostean fish have shown that migrating deep cells follow rather behind the expanding edges of the Ysl and the enveloping layer (Evl) (e.g. BETCHAKU & TRINKAUS 1978, WARGA & KIMMEL 1990). The deep cells of the blastoderm then fill in the space between the Ysl and the Evl as epiboly proceeds. The deep blastomeres lying between these two layers in *P. isidori* also move over the surface of the yolk to envelop it completely.

The teleost gastrulation starts during epiboly when the moving edge of the deep cells involutes, causing a marginal thickening termed germ ring (OPPENHEIMER 1936, PASTEELS 1936, BALLARD 1973, HISAOKA & BATTLE 1958, TRINKAUS & ERICKSON 1983, WOOD & TIMMERMAN 1988). During gastrulation the cells in the germ

ring converge towards the dorsal side, where they accumulate and form the embryonic shield which gives rise to the embryo (OPPENHEIMER 1936, PASTEELS 1936, BALLARD 1973, TRINKAUS & ERICKSON 1983).

The extent to which the blastoderm has spread over the yolk at the moment of embryonic shield formation, just preceding the onset of gastrulation, is variable within teleosts. In *P. isidori* a well developed germ ring and a thick shield are already established when the blastoderm covers around 20% of the yolk cell. In the substrate-breeding cichlid, e.g. *Cichlasoma dimerus* (see MEIJIDE & GUERRERO 2000), in mouth-breeding cichlid, e.g. *Haplochromis* 'velvet black' and *H. nyererei* (FLEIG 1993), as well as in the trout *Oncorhynchus gairdneri* (BALLARD 1973) gastrulation starts somewhat later, at around 30% yolk coverage. In *Fundulus heteroclitus* (Cyprinodontiformes; BETCHAKU & TRINKAUS 1978) and in *Barbus conchoni* (WOOD & TIMMERMAN 1988, GEVERS & TIMMERMAN 1991), gastrulation only starts when blastoderm covers 50% of the yolk cell.

At almost one third of the blastoderm spreading, deep cells from the anteroventral side of the blastoderm, in the vicinity of the original animal polar region, migrate rapidly by epiboly and converge toward the lengthening embryonic axis, leaving an empty large space the evacuation zone (BALLARD 1981, 1986). A tiny evacuation zone is demonstrated in *Danio rerio* (KIMMEL et al. 1995), and in the walleye, the percid *Stizostedion vitreum*, it is more conspicuously visible. In addition to the differences of the egg mentioned above, *P. isidori* is clearly distinguished from *Mormyrus rume probosciostris* by several aspects of external morphology in early ontogenetic stages already. The germ ring of *M. rume probosciostris* is about double the height as compared to *P. isidori* (own observation). The evacuation zone of the former species is larger and extends much further into the epidermal yolk sac cover. This evacuation zone persists in *M. rume probosciostris* until the end of epiboly and a remnant of a yolk plug was often observed. In *P. isidori* the evacuation zone disappears earlier without any trace and the yolk



cell becomes wholly encompassed by the blastoderm. The region of the epidermal yolk sac surrounding the blastopore is free of yolk syncytial nuclei (Ysn) in *M. rume probosciostris*, whereas in *P. isidori* this region is largely covered by scattered Ysn of the Ysl.

Externally, neurulation in *P. isidori* seems to occur in much the same way as it does in amphibians or *Polypterus senegalus*; but, in contrast to these, the neural folds are much less prominent and form a non tubular thickened tissue often called a neural keel. LANGLAND & KIMMEL (1997) reported that, in "fish", the keel gradually rounds up into a solid neural rod (and not a neural tube), which then forms a hollow core and tube-like structure later on. Very prominent and very early in development of Mormyridae is the formation of the large cerebellum. It is recognized from stage 28 onwards, shortly after hatching in *P. isidori* as well as in *P. adspersus*. This corresponds to the formation of a larval electrical organ, which becomes functional in about 7 mm long free embryos (stage 32, 7-8 days old) and is a distinct difference to all other Osteoglossomorpha and most Teleostei. HAUGÉDÉ-CARRÉ et al. (1979) state that the ontogenetic study of the gigantocerebellum of *Pollimyrus adspersus* confirms the conclusion from comparative anatomical investigations of previous workers, according to which the huge mormyrid brain is the result of the cerebellar hypertrophy. This hypertrophy is due principally to the extraordinary volume of the valvula, which covers the corpus cerebelli and almost the whole dorsal and dorso-lateral brain surface (see SANDERS 1882, HAUGÉDÉ-CARRÉ et al. 1979). As NIEUWENHUY (1967) has pointed out for *Gnathonemus sp.*, the corpus cerebelli in *Pollimyrus adspersus* (HAUGÉDÉ-CARRÉ et al. 1979) and *P. isidori* (this study) also possesses several lobes not typical of the teleost cerebellum, occupying the centre of the brain and pushed frontally by the hypertrophied acustico-lateralis area.

At hatching, many organ systems are still absent or incomplete in mormyrids, and organogenesis continues at a rapid pace until the yolk is exhausted and active feeding starts.

The hatched free embryo of *P. isidori* measures 3.4 mm; this is almost the same size as in *P. adspersus*. In both species, the hatching free embryos present a club-shaped appearance with a spherical yolk sac and a globular, voluminous head. The eyes are not pigmented, the mouth is not open. In *M. rume probosciostris* the head of the hatched free embryo is slightly lifted dorsally, with a flat and pointed anterior part, and its eyes are heavily pigmented.

Concerning other osteoglossomorphs, for *Pantodon buchholzi* it is reported that the embryos hatch on the third day (at 29 °C) after egg deposition. Free embryos measure 4.2-4.6 mm (BRITZ 2004). The most prominent structure on the head are the massive and protruding lower jaw processes which are equipped with a bony tooth-like structure that is continuous with the developing dentary; no true jaw teeth are developed yet. Moreover, the illustrated free embryo shows pigmented eyes, olfactory nostrils, and large opercular openings. The assumed immediate post-hatching condition in the free embryo of the presumably most basal group of osteoglossomorphs shows developed visceral arches and a further detached anterior part of the head from the yolk sac according to the description of BATTLE & SPRULES (1960) of *Hiodon alosoides*. In the *H. tergisus* specimen illustrated by FISH (1932), the terminal mouth is open, pectoral fins are well developed, though without rays, and in the caudal fin dermal rays are developing ventral to the notochord already. Based on the smallest (7.1 mm) free embryo examined by SNYDER & DOUGLAS (1978), however, neither the stomodeum nor the pectoral fin buds are evident in just-hatched free embryos. At least some minimal functional development of the eye is inferred to be important for free embryos, particularly of those species that lack parental care. Evidence for this interpretation comes from the observation that species of mormyrids that lack eye pigment at hatching exhibit parental care, whereas pigmented eyes at hatching are present in non-guarders such as *M. rume probosciostris*.

Very late in the free-embryonic phase, differentiation of the caudal fin rays in *P. isidori* as



well as in *P. adspersus* leads first to a pointed caudal fin before emergence of the borderline indicating the onset of dichotomization of the caudal fin into upper and lower lobes. This feature is never observed in *M. rume probosciostris* and *Hippopotamyrus pictus* (personal observations; cf. SCHUGARDT & KIRSCHBAUM 1996, 1998, 2006). In *Hippopotamyrus pictus*, the caudal fin starts to dichotomize from a roundish and notched end in the free embryo.

Immediately before onset of exogenous feeding, simultaneous emergence of both, swim bladder and otic vesicle in *P. isidori* (present study) and in *M. rume probosciostris* (personal observation) are noticed macroscopically. The joint emergence of the otic vesicle and swim bladder are also demonstrated in *P. adspersus* and *Campylomormyrus tamandua* (KIRSCHBAUM & SCHUGARDT 2002). These structures are, at least externally, not visible in *Petrocephalus soudanensis* before onset of feeding. The development of the dorsal and anal fins begins before onset of exogenous feeding in *P. isidori*, *P. adspersus* and *M. rume probosciostris*. In *Campylomormyrus tamandua*, *Petrocephalus soudanensis* and *Hippopotamyrus pictus* the differentiation of the dorsal and anal fins occurs first in the larval period.

In Mormyridae the anal and dorsal fins emerge simultaneously after the caudal and pectoral fins, and largely prior to the appearance of the pelvic fins, which form at the time of complete regression of the membranous preanal embryonic fin fold. The sequence of formation of the fins in *Pantodon buchholzi* according to MOHN (1976 b) occurs after hatching in the following manner: first day the pectoral fin is clearly visible, the caudal and anal fins appear, then the pelvic fin at the 14<sup>th</sup> day and finally the dorsal fin at the 16<sup>th</sup> day. In contrast to MOHN (1976 b), BRITZ (2004) presents a different scheme in the order of appearance of the fins based on the total length of the (yolk-sac) larvae: two to three fin rays are developed in the caudal at day one after hatching. At 7.5 mm, the first anal fin rays appear, at 8.0-8.5 mm the pectoral can be recognized, the dorsal fin rays begin to develop at around 9.5 mm, and the pelvic fins are the last to appear. Based on the

early and late larvae of *Hiodon tergisus* illustrated in SNYDER & DOUGLAS (1978), the fins seem to form according to an identical chronology (not in the absolute timing) as described in the present study in *P. isidori*. In contrast to *P. isidori*, in which the pelvic fins develop when the ventral fin fold is almost completely regressed, in *H. tergisus* conspicuous pelvic fin buds are observed already, when no significant reduction of the ventral fin fold has occurred. The figures of 'mesolarvae' of *H. alosoides* (BATTLE & SPRULES 1960) demonstrate clearly the successive emergence of the fins in the following sequence instead: Pectoral, caudal, anal, dorsal, and pelvic. This leaves the matter of the ancestral pattern of Osteoglossomorpha a bit doubtful again.

Very late in the finformed larva, almost a juvenile, external morphological traits are sufficient to separate *Pollimyrus isidori* and *P. adspersus* on the basis of two characters utilized in the differential diagnoses of the adults (DIEDHIOU et al. 2007): (1) the end of the anal fin extends beyond the end of the dorsal fin in *P. adspersus*; in *P. isidori* these two unpaired fins end nearly at the same level, (2) *P. adspersus* has a higher relative body depth than *P. isidori* as seen in the relationship standard length versus depth of the body at the beginning of the anal and dorsal fins, whereas the depth of the caudal peduncle is higher in *P. isidori* than in *P. adspersus*, both when compared to standard length or body depth.

#### 4.3 Melanophore pattern

First melanophores appear in *Pollimyrus isidori*, in the dorsal head epidermis, during the day after hatching. SNYDER & DOUGLAS (1978) reported that a few days after hatching *Hiodon tergisus* shows just some branched melanophores, distributed on the ventral half of the yolk sac. In contrast to *H. tergisus*, up to 13.5 mm length, the semi-transparent, free embryo of *H. alosoides* (BATTLE & SPRULES 1960) usually lacks melanophores completely. But, occasionally exceptions may occur, where melanophores appear on the mid-dorsal surface of the early free embryo of *H. alosoides* already. In



*Pantodon buchholzi* (BRITZ 2004) the depicted 24 hours old tail bud embryo, assumed to correspond to stage 25 of *P. isidori*, shows already blackish melanophore areas on the head and body and a reticulate pattern on the dorsal region of the yolk-sac; clearly, this pigmentation is developed well before. Early pigmentation or lack of pigmentation may play an important role in the camouflage of embryos and larvae among plants and roots or in the free water column, respectively. At least some populations of *P. isidori* and *P. adspersus* are easily distinguished as juveniles by coloration, the former species usually showing larger, scattered melanophores on a lighter background, against a more evenly distributed dark pigment in the latter (cf. DIEDHIOU et al. 2007).

## 5. Conclusion

There is a wealth of early ontogenetic adaptation, variants and reproductive strategies apparently realized among Osteoglossomorpha that are not easily brought into a phylogenetic scheme. Several modes of parental care have evolved independently. There are several reproductive guilds represented in this order. The two *Pollimyrus* species can be characterized more precisely as guarders and clutch tenders with rather high fecundity according to current schemes of reproductive strategies (cf. LÉVÊQUE 1997). Among Mormyridae, in the studied species *P. isidori* (as well as in the closely related *P. adspersus* (KIRSCHBAUM 1987), parental care, small size at hatching or reduced/shortened phase of intrachorionic embryonic development are somehow reflected in several characters of early ontogeny and timing of morphogenetic events.

## Acknowledgements

We wish to thank Dr. Timo MORITZ for providing the life adult specimens of *Pollimyrus isidori* from Bougouriba River. Prof. Dr. Ulrich ZELLER and Gabriele DRESCHER are thankfully acknowledged for permission of access and help with the SEM-technique for study of the blastula and onset of epiboly. Anonymous re-

viewer and the editor, Prof. Dr. Hartmut GREVEN, are thankfully acknowledged for critically reading and correcting the manuscript.

## Literature

- ASSHETON, R. 1907. The development of *Gymnarchus niloticus*, pp. 293-421. In: Budgett Memorial Volume (KERR, J.G., ed). Cambridge, London.
- AXELROD, H.R., & W.E. BURGESS. 1981. Spawning *Notopterus notopterus*. Tropical Fish Hobbyist 29, 38-49.
- AZUMA, H. 1998. Breeding the gold Asian arowana. Tropical Fish Hobbyist 40, 10-12; 14, 19-20, 22-23.
- BALLARD, W.W. 1973. A new fate map for *Salmo gairdneri*. Journal of Experimental Zoology 184, 49-74.
- BALLARD, W.W. 1981. Morphogenetic movements and fate maps of vertebrates. American Zoologist 21, 391-399.
- BALLARD, W.W. 1986. Morphogenetic movements and a provisional fate map of development in the holostean fish *Amia calva*. Journal of Experimental Zoology 238, 355-372.
- BALON, E.K. 1975. Terminology of intervals in fish development. Journal of the Fisheries Research Board of Canada 32, 1663-1670.
- BALON, E.K. 1985. The theory of saltatory ontogeny and life history models revisited, pp. 13-31. In: Developments in environmental biology of fishes: Early life histories of fishes (BALON, E.K., ed). W. Junk, Dordrecht.
- BALON, E.K. 1999. Alternative ways to become a juvenile or a definitive phenotype (and on some persisting linguistic offenses). Environmental Biology of Fishes 56, 17-38.
- BALON, E.K. 2002. Epigenetic processes, when natura non facit saltum becomes a mythe, and alternative ontogenies a mechanism of evolution. Environmental Biology of Fishes 65, 1-32.
- BARTSCH, P., S. GEMBALLA, & T. PIOTROWSKI. 1997. The embryonic and larval development of *Polypterus senegalus* Cuvier, 1829: its staging with reference to external and skeletal features, behaviour and locomotory habits. Acta Zoologica 78, 309-328.
- BATTLE, H.I., & W.M. SPRULES. 1960. A description of the semi-buoyant eggs and early development stage of the goldeye, *Hiodon alosoides* (Rafinesque). Journal of the Fisheries Research Board of Canada 17, 245-266.
- BETCHAKU, T., & J.P. TRINKAUS. 1978. Contact relations, surface activity, and cortical microfilaments of marginal cells of the enveloping layer and of the yolk syncytial and yolk cytoplasmic layers of



- Fundulus* before and during epiboly. Journal of Experimental Zoology 206, 381-426.
- BREDER, C.M., & D.E. ROSEN. 1966. Modes of reproduction in fishes. TFH, New Jersey.
- BRITZ, R. 2004. Egg structure and larval development of *Pantodon buchholzi* (Teleostei: Osteoglossomorpha), with a review of the data on reproduction and early life history in the other osteoglossomorphs. Ichthyological Exploration of Freshwaters 15, 209-224.
- BUDGETT, J.S. 1901. On the breeding habits of some West-African fishes, with an account of the external features in the development of *Protopterus annectens*, and a description of the larva of *Polypterus lapradei*. Transaction of the Zoological Society of London 16, 115-136.
- CRAWFORD, J. D., M. HAGEDORN & C. D. HOPKINS. 1986. Acoustic communication in an electric fish *Pollimyrus isidori* (Mormyridae). Journal of Comparative Physiology 100, 3-14.
- DAGET, J. 1957. Mémoires sur la biologie des poissons du Niger moyen. III. Reproduction et croissance d'*Heterotis niloticus* Ehrenberg. Bulletin de l'Institut Français d'Afrique Noire 19, 295-323.
- DIEDHILOU, S., T. MORTIZ, P. BARTSCH, & F. KIRSCHBAUM. 2007. Comparison of *Pollimyrus isidori* and *Pollimyrus adspersus* (Mormyridae) based on morphometric, meristic, ontogenetic, and physiological characteristics. Bulletin of Fish Biology 9, 13-25.
- FISH, M.P. 1932. Contributions to the early life histories of the species of fishes from Lake Erie and its tributary waters. Bulletin of the United States Bureau of Fisheries 47, 293-298.
- FLEIG, R. 1993. Embryogenesis in mouth-breeding cichlids (Osteichthyes, Teleostei): Structure and fate of the enveloping layer. Development Genes and Evolution. 230, 124-130.
- FONTENELE, O. 1948. Contribuição para o conhecimento da biologia do Pirarucu, "*Arapaima gigas*" (Cuvier), em cativo (Actinopterygii, Osteoglossidae). Revista Brasileira de Biologia 8, 445-459.
- FONTENELE, O. 1952. Habitos de desova do Pirarucu, "*Arapaima gigas*" (Cuvier) (Pisces: Isopsondyli, Arapaimidae), e evolução de sua larva. Ministério da Viação e Obras Publicas, Departamento Nacional de Obras contra as Secas Serviço de Piscicultura, Publicação 153, 1-22.
- GEVERS, P., & D.P.M. TIMMERMANS. 1991. Dye-coupling and the formation and fate of the hypoblast in the teleost fish embryo, *Barbus conchoniis*. Development 112, 431-438.
- GOSSE, J.P. 1984. Mormyridae, Gymnotidae, pp. 63-124. In: Checklist of the freshwater fishes of Africa (CLOFFA) (DAGET, J., J.P. Gosse, & D.F.E. VAN DEN AUDENAERDE, eds). Vol. 1, ORSTOM and MRAC, Tervuren.
- HAUGÉDÉ-CARRÉ, F., T. SZABO, & F. KIRSCHBAUM. 1979. Development of the gigantocerebellum of the weakly electric fish *Pollimyrus*. Journal de Physiologie 75, 381-395.
- HERMENS, M., M. DAFÉ, & P. VANDELLE. 2007. Observations of the reduction of external gill filaments during larval development in *Heterotis niloticus*. Belgian Journal of Zoology 137, 247-249.
- HILTON, E.J. 2003. Comparative osteology and phylogenetic systematics of fossil and living bony-tongue fishes (Actinopterygii, Teleostei, Osteoglossomorpha). Zoological Journal of the Linnean Society 137, 1-100.
- HISAOKA, K.K., & H.I. BATTLE. 1958. The normal developmental stages of the zebrafish, *Brachydanio rerio* (Hamilton Buchanan). Journal of Morphology 102, 311-328.
- JOHNELS, A.G. 1954. Notes on fishes from the Gambia River. Arkiv foer Zoologi 6, 327-411.
- JOHNSON, E.Z., & R.G. WERNER. 1986. Scanning electron microscopy of the chorion of selected freshwater fishes. Journal of Fish Biology 29, 257-265.
- KIMMEL, C.B., W.W. BALLARD, S.R. KIMMEL, B. ULLMANN, & T.F. SCHILLING. 1995. Stages of embryonic development of zebrafish. Developmental Dynamics 203, 253-310.
- KIMMEL, C.B., & R.D. LAW. 1985. Cell lineage of zebrafish blastomeres. II. Formation of the yolk syncytial layer. Developmental Biology 108, 86-93.
- KIRSCHBAUM, F. 1987. Reproduction and development of the weakly electric fish, *Pollimyrus isidori* (Mormyridae, Teleostei) in captivity. Environmental Biology of Fishes 20, 11-31.
- KIRSCHBAUM, F. 2006. Erstmalige Zucht eines Vertreters der Nilhechtgattung *Petrocephalus* (*P. soudanensis*) induziert durch Imitation von Hochwasserbedingungen, pp. 65-70. In: Biologie der Aquarienfische (GREVEN, H., & R. RIEHL, eds). Tetra Verlag GmbH, Berlin-Veltn.
- KIRSCHBAUM, F., & C. SCHUGARDT. 1995. Vergleichende Daten zur Fortpflanzungsbiologie von zwei Nilhecht-Arten (Mormyridae), pp. 81-90. In: Fortpflanzungsbiologie der Aquarienfische (GREVEN, H., & R. RIEHL, eds). Birgit Schmettkamp Verlag, Bornheim.
- KIRSCHBAUM, F., & C. SCHUGARDT. 2002a. Reproductive strategies and development aspects in mormyrid and Gymnotiform fishes. Journal of Physiology 96, 557-566.



- KIRSCHBAUM, F., & C. SCHUGARDT. 2002b. Erstmalige Zucht eines Vertreters der Nilhechtgattung *Hippopotamyrus* (*H. pictus*) durch Imitation von Hochwasserbedingungen, pp. 91-97. In: Verhalten der Aquarienfische (RIEHL, R., & H. GREVEN, eds). Birgit Schmettkamp Verlag, Bornheim.
- KIRSCHBAUM, F., & C. SCHUGARDT. 2006. Fortpflanzungsstrategien und entwicklungsbiologische Aspekte bei südamerikanischen Messerfischen (Gymnotiformes) und afrikanischen Nilhechten (Mormyridae) – vergleichende Betrachtungen, pp. 81-116. In: Biologie der Aquarienfische (GREVEN, H., & R. RIEHL, eds). Tetra Verlag, Berlin.
- LAKE, J.S., & S.H. MIDGLEY. 1970. Australian Osteoglossidae (Teleostei). Australian Journal of Science 32, 442-443.
- LANGLAND, J.A., & C.B. KIMMEL. 1997. Fishes, pp. 383-407. In: Embryology constructing the organism (GILBERT S.F., A.M. RAUNO, & M.A. SUNDERLAND, eds). Sinauer Associates.
- LÉVÊQUE, C. 1997. Biodiversity dynamics and conservation: The Freshwater Fish of Tropical Africa. Cambridge University, New York.
- LONG, W.L. 1984. Cell movements in teleost fish development. BioScience 2, 84-88.
- LONG, W.L. 2005. The role of the yolk syncytial layer in determination of the plane of bilateral symmetry in the rainbow trout, *Salmo gairdneri* Richardson. Journal of Experimental Zoology. 228, 91-97.
- LÜLING, K.H. 1964. Zur Biologie und Ökologie von *Arapaima gigas* (Pisces, Osteoglossidae). Zeitschrift für Morphologie und Ökologie der Tiere 54, 436-530.
- LÜLING, K.H. 1969. Das Laichverhalten der Vertreter der Familie Osteoglossidae (Versuch einer Übersicht). Bonner Zoologische Beiträge 20, 228-243.
- MCELMAN, J.F., & E.K. BALON. 1979. Early ontogeny of walleye, *Stizostedion vitreum*, with steps of saltatory development. Environmental Biology of Fishes 4, 309-348.
- MEIJIDE, F.J., & G.A. GUERRERO. 2000. Embryonic and larval development of a substrate-brooding cichlid *Cichlasoma dimernus* (Heckel, 1840) under laboratory conditions. Journal of Zoology (London) 252, 481-495.
- MERREICK, R.S., & L.C. GREEN. 1982. Pont culture of the spotted barramundi, *Scleropages leichardti* (Pisces: Osteoglossidae). Aquaculture. 29, 171-176.
- MOHN, G. 1976a. Zur Haltung und Zucht des Schmetterlingsfisches, *Pantodon buchholzi* 1. Aquarien Terrarien 23, 342-344.
- MOHN, G. 1976b. Zur Haltung und Zucht des Schmetterlingsfisches, *Pantodon buchholzi* 2. Aquarien Terrarien 23, 372-375.
- MOOKERJEE, H.K., & S.R. MAJUMDAR. 1946. On the life history of *Notopterus notopterus* (Pallas). Journal of the Department of Sciences of the Calcutta University 2, 88-100.
- NEVES, A.M.B. 1998. Conhecimento atual sobre o piracuru, *Arapaima gigas* (Cuvier, 1817). Boletim do Museu Paraense Emilio Goeldi 11, 33-56.
- NIEUWENHUIS, R. 1967. Comparative anatomy of the cerebellum, pp. 1-93. In: Progress in brain research (FOX, C.A., & R.S. SNEIDER, eds). Amsterdam, Elsevier.
- OPPENHEIMER, J.M. 1936. Process of localization in developing *Fundulus*. Journal of Experimental Zoology 73, 405-44.
- PASTEELS, J. 1936. Etudes sur la gastrulation des vertébrés méroblastiques. I. Téléostéens. Archive de Biology 47, 205-308.
- RIEHL, R. 1996. The ecological significance of the egg envelope in teleosts with special reference to limnic species. Limnologia 26, 183-189.
- RIZZO, E., Y. SATO, B.P. BARRETO, & H.P. GODINHO. 2002. Adhesiveness and surface patterns of eggs in neotropical freshwater teleosts. Journal of Fish Biology 61, 615-632.
- SANDERS, A. 1882. Contribution to the anatomy of the central nervous system in vertebrate animals. Appendix: On the brain of the mormyridae. Philosophical Transactions of the Royal Society of London 173, 927-959.
- SCHUGARDT, C., & F. KIRSCHBAUM. 1996. Daten zur Fortpflanzungsbiologie des Nilhechtes *Mormyrus rume probosciostris* (Boulenger, 1898) unter experimentellen Bedingungen. Deutsche Gesellschaft für Limnologie, Jahrestagung in Berlin, 24.-29. September 1995, erweiterte Zusammenfassung, 833-837.
- SCHUGARDT, C., & F. KIRSCHBAUM. 1998. Sozial- und Fortpflanzungsverhalten von Mormyriden, pp. 87-98. In: Verhalten der Aquarienfische (GREVEN H., & R. RIEHL, eds). Birgit Schmettkamp Verlag, Bornheim.
- SCHUGARDT, C., & F. KIRSCHBAUM. 2004. Control of gonad maturation and regression by experimental variation of environmental factors in the mormyrid fish *Mormyrus rume probosciostris*. Environmental Biology of Fishes 70, 227-233.
- SCHUGARDT, C., & F. KIRSCHBAUM. 2006. Erstmaliges Abbläichen der zwei Nilhechte *Mormyrus* sp. und *Marcusenius mento* unter Aquarienbedingungen, induziert durch Imitation von Hochwasserbedingungen, pp. 159-169. In: Biologie der Aquarienfische (GREVEN H., & R. RIEHL, eds). Tetra Verlag, Berlin.



- SHADO, J.D. 1995. Comparative embryology of teleostean fishes. I. development and staging of american shad, *Alosa sapidissima* (Wilson, 1811). *Journal of Morphology* 225, 125-167.
- SMITH, H.M. 1933. Contributions to the ichthyology of siam. VII. The featherback fish *Notopterus chitala* in siam with notes in its egg-laying and young. *Journal of the Siam Society* 9, 245-258.
- SNYDER, D.E., & S.C. DOUGLAS. 1978. Description and identification of mooneye, *Hiodon tergisus*, proto-larvae. *Transactions of the American Fisheries Society* 107, 590-594.
- SOUTHWELL, T., & B. PRASHAD. 1919. Notes from the Bengal fisheries laboratory, No. 6: Embryological and developmental studies of Indian fishes. *Records of the Indian Museum* 16, 215-240.
- SVENSSON, G.S.O. 1933. Fresh water fishes from the Gambia River (British West Africa). Results of the Swedish Expedition 1931. *Kungliga Svenska Vetenskapsakademiens Handlingar* 12, 1-102.
- TRINKAUS, J.P. 1984. Mechanisms of *Fundulus* epiboly. A current review. *American Zoologist* 24, 673-688.
- TRINKAUS, J.P. 1992. The midblastula transition, the YSL transition and the onset of gastrulation in *Fundulus*. *Development* supplement, 75-80.
- TRINKAUS, J.P. 1993. The yolk syncytial layer of *Fundulus*: its origin and history and its significance for early embryogenesis. *Journal of Experimental Zoology* 265, 258-284.
- TRINKAUS, J.P., & C.A. ERICKSON. 1983. Protrusive activity, mode and rate of locomotion, and pattern of adhesion of *Fundulus* deep cells during gastrulation. *Journal of Experimental Zoology* 228, 41-70.
- TRINKAUS, J.P., & T.L. LENTZ. 1967. Surface specializations of *Fundulus* cells and their relation to cell movements during gastrulation. *Journal of Cell Biology* 32, 139-153.
- UNGAR, C. 1993. Über die Zucht von *Osteoglossum bicirrhosum*. *Zoologischer Garten (N.F.)* 63, 329-334.
- WARGA, R.M., & C.B. KIMMEL. 1990. Cell movements during epiboly and gastrulation in zebrafish. *Development* 108, 569-580.
- WOLFSHEIMER, G. 1964. Arowanas spawned. *Aquarium Journal (San Francisco)* 35, 529-535.
- WOOD, A., & L.P.D. TIMMERMANS. 1988. Teleost epiboly of deep cell movement in the germ ring. *Development* 102, 575-585.

Received: 28.11.2007

Accepted: 11.12.2007